

Cu-tpa MOF derived electrocatalyst for oxygen reduction reaction with low Pt loading



By

Rehan Anwar

Reg # 170877

Session 2016-18

Supervised by

Assoc. Prof. Naseem Iqbal

**A Thesis Submitted to the US-Pakistan Center for
Advanced Studies in Energy in partial fulfillment of the
requirements for the degree of
MASTERS of SCIENCE in
Energy Systems Engineering**

US-Pakistan Center for Advanced Studies in Energy (USPCAS-E)

National University of Sciences and Technology (NUST)

H-12, Islamabad 44000, Pakistan

May 2019

Cu-tpa MOF derived electrocatalyst for oxygen reduction reaction with low Pt loading



By

Rehan Anwar

Reg # 170877

Session 2016-18

Supervised by

Assoc. Prof. Naseem Iqbal

**A Thesis Submitted to the US-Pakistan Center for
Advanced Studies in Energy in partial fulfillment of the
requirements for the degree of
MASTERS of SCIENCE in
Energy Systems Engineering**

US-Pakistan Center for Advanced Studies in Energy (USPCAS-E)

National University of Sciences and Technology (NUST)

H-12, Islamabad 44000, Pakistan

May 2019

THESIS ACCEPTANCE CERTIFICATE

Certified that final copy of MS/MPhil thesis written by Mr. Rehan Anwar, (Registration No. 170877), of US-Pakistan Center for Advanced Studies in Energy (USPCAS-E) has been vetted by undersigned, found complete in all respects as per NUST Statues/Regulations, is within the similarity indices limit and is accepted as partial fulfillment for the award of MS/MPhil degree. It is further certified that necessary amendments as pointed out by GEC members of the scholar have also been incorporated in the said thesis.

Signature: _____

Name of Supervisor Dr. Naseem Iqbal

Date: _____

Signature (HoD): _____

Date: _____

Signature (Dean/Principal): _____

Date: _____

Certificate

This is to certify that work in this thesis has been carried out by **Mr. Rehan Anwar** and completed under my supervision in Energy Storage and Conservation laboratory, US-Pakistan Center for Advanced Studies in Energy (USPCAS-E), National University of Sciences and Technology, H-12, Islamabad, Pakistan.

Supervisor:

Dr. Naseem Iqbal
USPCAS-E
NUST, Islamabad

GEC member # 1:

Dr. Majid Ali
USPCAS-E
NUST, Islamabad

GEC member # 2:

Dr. Nadia Shahzad
USPCAS-E
NUST, Islamabad

GEC member # 3:

Dr. Muhammad Zubair
USPCAS-E
NUST, Islamabad

HoD- (ESE)

Dr. Naseem Iqbal
USPCAS-E
NUST, Islamabad

Principal/ Dean

Dr. Zuhair S. Khan
USPCAS-E
NUST, Islamabad

Dedicated to my elder brother Lukman Anwar.

Abstract

Metal-organic frameworks (MOFs) have received special attention in the recent past because of their structural properties and wide applications in catalysis. MOFs are also used as hard templates for the preparation of catalysts. In this study, highly active CuPt/NC electrocatalyst was synthesized by pyrolyzing Cu-tpa MOF along with Pt precursor under flowing Ar-H₂ atmosphere. The catalyst was characterized by scanning electron microscopy (SEM), Transmission electron microscopy (TEM), X-ray photoelectron spectroscopy (XPS) and X-ray Powder Diffraction (XRD). Rotating disk electrode study was performed to determine the oxygen reduction reaction (ORR) activity for CuPt/NC in 0.1 M HClO₄ at different rotation (400, 800, 1200 and 1600rpm) and also compared with commercial Pt/C catalyst. CuPt/NC shows excellent ORR performance with onset potential of 0.9V (vs. RHE) and half wave potential of 0.79V (vs. RHE), which is comparable with commercial Pt/C. The ORR activity of CuPt/NC exhibited it as an efficient electrocatalyst for fuel cell technology.

Keywords: Cu-tpa MOF; PEMFC ORR electrocatalyst; CuPt/NC; Platinum

Table of Contents	
Abstract	i
List of figures	v
List of tables	vii
List of Journals/Conference Papers	viii
List of Abbreviations	ix
Chapter 1 Introduction	1
1.1 Introduction to fuel cells	1
1.2 Working Principle of PEMFC	2
1.3 Fuel Cell Performance	3
1.4 Membrane Electrode Assembly	4
1.5 Challenges for the commercialization of PEMFC	5
Summary:	6
References	7
Chapter 2 Literature Review	9
2.1 Recent developments in oxygen reduction reaction	9
2.2 Introduction to Oxygen Reduction Reaction	9
2.2.1 Electrochemical Oxygen Reduction Reaction	9
2.2.2 ORR Mechanism	11
2.2.3 ORR mechanism on Pt-electrode	11
2.2.4 ORR mechanism on precious metal electrodes	12
2.3 Metal Organic Frameworks and electrocatalysis	13
Summary:	16
References	17
Chapter 3 Characterization	19
3.1 Physical Characterization	19
	ii

3.1.1	Scanning Electron Microscopy (SEM/EDS)	19
3.1.2	Transmission Electron Microscopy (TEM)	20
3.1.3	X-ray Photoelectron Spectroscopy (XPS)	20
3.1.4	X-ray diffraction (XRD)	21
3.1.5	Thermal Gravimetric Analysis (TGA)	22
3.1.6	Fourier Transform Infrared Spectroscopy (FTIR)	22
3.2	Electrochemical Characterization	23
3.2.1	Cyclic Voltammetry (CV)	23
3.2.2	Linear Sweep Voltammetry (LSV)	23
3.2.3	Electrochemical impedance spectroscopy (EIS)	24
	Summary:	25
	References	26
Chapter 4	Experimentation	27
4.1	Materials	27
4.2	Cu-tpa MOF synthesis	27
4.3	Synthesis of Cu/NC	28
4.4	Synthesis of CuPt/NC	28
4.5	Catalyst ink	29
4.6	Electrode preparation	29
4.7	Electrochemical setup	30
	Summary:	31
	References	32
Chapter 5	Results and discussion	33
5.1	Scanning electron microscopy (SEM) analysis of CuPt/NC	33
5.2	Transmission electron microscopy (TEM) analysis of CuPt/NC	33

5.3	X-ray diffraction (XRD) analysis of CuPt/NC	34
5.4	X-ray photoelectron spectroscopy (XPS) analysis of CuPt/NC	35
5.5	Electrochemical testing of CuPt/NC for ORR	35
	Summary	41
	References	42
Chapter 6	Conclusion and Recommendations	43
6.1	Conclusion	43
6.2	Recommendations	43
	Acknowledgments	44
	Annex	45

List of figures

Figure 1- 1 Working Principle of PEMFC.....	3
Figure 1- 2 Fuel Cell performance Curves.....	3
Figure 1- 3 Fuel cell components, Nth unit cell in a fuel cell stack, showing expanded MEA.....	4
Figure 2- 1 Schematic illustration of ORR kinetics	11
Figure 2- 2 Plot of ORR activity as function of M-O binding energy (a) and M-OH binding energies (b).....	12
Figure 3- 1 Working principle of SEM.....	19
Figure 3- 2 Schematic of TEM.....	20
Figure 3- 3 Basics of XPS.....	21
Figure 3- 4 XRD illustration	21
Figure 3- 5 Components of TGA	22
Figure 3- 6 Working principle of FTIR.....	22
Figure 3- 7 (a) basic CV plot (b) CV plot at multiple scan rates(mV/s).....	23
Figure 3- 8 (a) general LSV graph (b) LSV at multiple scan rates (mV/s).....	24
Figure 3- 9 EIS of randles circuit.....	24
Figure 4- 1 Synthesis of Cu-tpa MOF.....	27
Figure 4- 2 Cu-tpa MOF sample	28
Figure 4- 3 Synthesis of Cu/NC	28
Figure 4- 4 Synthesis of CuPt/NC.....	29
Figure 4- 5 CuPt/NC sample	29
Figure 4- 6 Glassy carbon electrode with ink deposited on it.....	30
Figure 5- 1 Scanning electron microscopy images of (a) Cu-tpa MOF (b) Cu/NC (c) CuPt/NC	33
Figure 5- 2 Transmission electron micrographs for CuPt/NC (a) 50nm (b) 20nm (c) 10nm	34
Figure 5- 3 XRD pattern of CuPt/NC	34
Figure 5- 4 XPS spectrum of CuPt/NC.....	35

Figure 5- 5 CV plots for CuPt/NC and commercial Pt/C.....	36
Figure 5- 6 CV plot for CuPt/NC with O ₂ and N ₂ saturation.....	37
Figure 5- 7 LSV measurements of CuPt/NC at different rpms.....	37
Figure 5- 8 LSV plots of CuPt/NC and commercial Pt/C at 1600 rpm with O ₂ saturation	37
Figure 5- 9 LSV measurements of CuPt/NC with O ₂ and N ₂ 1600rpm.....	38
Figure 5- 10 LSV plots of Cu/NC and CuPt/NC	39
Figure 5- 11 The nyquist plots of CuPt/NC and commercial Pt/C.....	39

List of tables

Table 1-1 Summary of the common types of fuel cells... ..	2
Table 2-1 Structures of MOFs according to the organic linker used	15

List of Journals/Conference Papers

1. **Rehan Anwar**, Saadia Hanif, Naseem Iqbal, Xuan Shi, Daarain Haider, Syed Aun M. Tayyaba Noor, A. M. Kannan “Low Platinum loaded Cu-MOF derived electrocatalyst for oxygen reduction reaction in polymer electrolyte membrane fuel cell” Conference: Energy Materials and Nanotechnology (15-16 August 2018)

List of Abbreviations

AC	Activated Carbon	LSV	Linear sweep Voltammetry
AFC	Alkaline fuel cell	MCFC	Molten Carbonate fuel cell
BET	Brunauer Emmett Teller	MEA	Membrane electrode assembly
BTC	Benzene tricarboxylic	MOF	Metal Organic Frameworks
CA	Chronoamperometry	OER	Oxygen Evaluation Reaction
CNTs	Carbon Nanotubes	ORR	Oxygen Reduction Reaction
CV	Cyclic Voltammetry	PAFC	Phosphoric Acid fuel cell
DI	Di-Ionized water	SEM	Scanning Electron Microscopy
DMFC	Direct Methanol fuel cell	SOFC	Solid Oxide fuel cell
DOE	Department of Energy	TGA	Thermal Gravimetric Analysis
EDS	Energy Dispersive Spectroscopy	RFC	Reversible fuel cell
EIS	Electronic Impedance Spectroscopy		
FC	Fuel cell		
FTIR	Fourier Transform Infrared Spectroscopy		
GCE	Glassy Carbon Electrode		
GDL	Gas diffusion layer		
HOR	Hydrogen Oxidation Reaction		
ICT	Internal Combustion Engine		
PEMFC	Polymer Electrolyte Membrane fuel cell		
XRD	X-ray Diffraction		

Chapter 1 Introduction

1.1 Introduction to fuel cells

The running down of fossil fuels and climate change led to the global energy transition from petroleum based energy resources to renewable energy resources [1,2]. From the past few decades fuel cell technologies have got special attention because of their low emissions and high efficiencies [3,4,5]. Generally, fuel cells use hydrogen or methanol as fuel which has almost zero carbon prints. Fuel cell is an energy conversion device that converts the chemical energy of fuels (H₂, Methanol) into electrical energy through electrochemical process [6]. Battery also use electrochemical process to produce electricity, however, fuel cell requires continuous supply of fuel and oxidant unlike in battery. In fuel cell electrodes do not undergo chemical changes but in battery they do [7].

Fuel cells have seven categories as defined by DOE [8]:

1. Phosphoric acid fuel cell (PAFC)
2. Polymer electrolyte membrane fuel cell (PEMFC)
3. Molten carbonate fuel cell (MCFC)
4. Alkaline fuel cell (AFC)
5. Solid-oxide fuel cell (SOFC)
6. Reversible fuel cell (RFC)
7. Direct methanol fuel cell (DMFC)

Table 1-1 shows the major types of fuel cell along with the electrolyte used it them, cell components, catalyst, operating temperature, and fuel compatibility [9]. Among all these types PEMFC and DMFC are considered the most potential power sources due to their lower operating temperature, higher efficiencies, quick start-up, and lesser environmental impacts [10]. In this present study, only PMFC will be considered and the main focus will be on the cathode side reaction in fuel cell which is oxygen reduction reaction (ORR).

	PEMFC	MCFC	PAFC	AFC	SOFC	DMFC
Electrolyte	Polymer membrane	Molten carbonates	Liquid H ₃ PO ₄	Liquid KOH	Ceramic	Polymer membrane
Charge carrier	H ⁺	CO ₃ ²⁻	H ⁺	OH ⁻	O ⁻²	H ⁺
Operating temperature	80°C	650°C	200°C	60-220°C	600-1000°C	80°C
Catalyst	Pt	Ni	Pt	Pt	Perovskites (ceramic)	Pt
Cell components	Carbon Based	Stainless based	Carbon based	Carbon based	Ceramic based	Carbon based
Fuel compatibility	Hydrogen, methanol	Hydrogen, Methane	Hydrogen	Hydrogen	H ₂ , CH ₄ , CO	Methanol

Table 1-1 Summary of the common types of fuel cells [7].

1.2 Working Principle of PEMFC

A simplified schematic is shown in Figure 1-1, which explains the working of PEMFC along with its components. The oxidation of H₂ occurs at anode and, the reduction of O₂ takes place at cathode as a result of this redox reaction water is produced [11]. The flow of electrons involve in the redox reaction from anode to cathode through an external circuit produce electricity. The membrane (electrolyte) is responsible for the transport of protons from anode to cathode [12,13]. The complete redox reaction is shown below with hydrogen as oxidizing specie and oxygen as reducing specie:



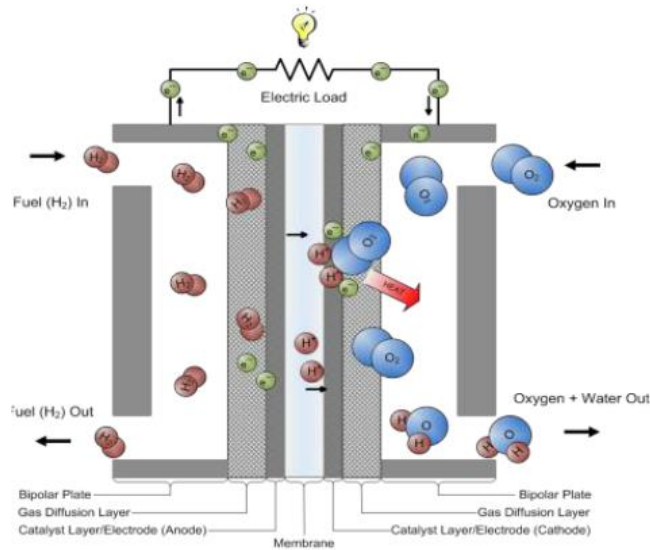


Figure 1- 1 Working Principle of PEMFC

1.3 Fuel Cell Performance

I-V characteristic (or polarization curve) summarizes the fuel cell performance. A perfect fuel cell should supply any amount of current while maintaining the voltage at constant value but in real time systems as the amount of current increases the voltage decreases. The lower value of actual voltage is explained by the types of losses in fuel cell ideal voltage due to three types of losses: ohmic losses, activation losses, and mass transportation losses, reasons for all three losses are slow kinetics, electrical resistance offered by cell components, resistance in reactant and product mass flows respectively. Figure 1-2 shows the combined fuel cell I-V and polarization curve [7].

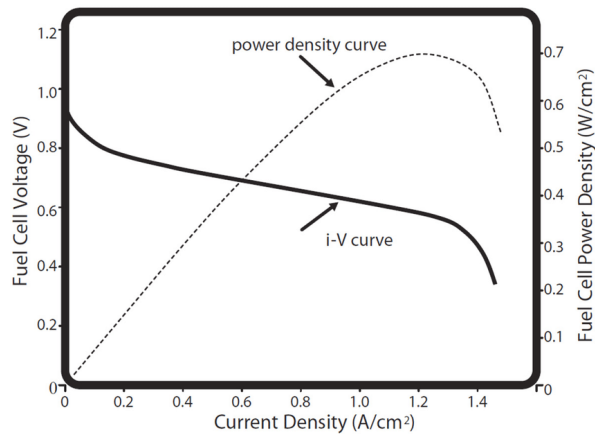


Figure 1- 2 Fuel Cell performance Curves

1.4 Membrane Electrode Assembly

Membrane electrode assembly also known as MEA which is the core of PEMFC. Figure 1-3 illustrates a unit cell from a fuel cell stack with all the component of PEMFC. MEA is responsible for the oxidation and reduction reactions occur at anode and cathode respectively. The hydrogen oxidation reaction (HOR) and oxygen reduction reaction (ORR) both reactions take place on Pt-based electrodes. Water and heat are the only byproducts in these reactions. Membrane present between the electrodes only conducts the H^+ ions. The function of bipolar plates is to compress the MEA, provide gases flow channels, and harvesting of electric current produces in the process. Gas diffusion layers (GDL) are responsible for the transport of reactants and product water between the electrodes and gases flow fields [10].

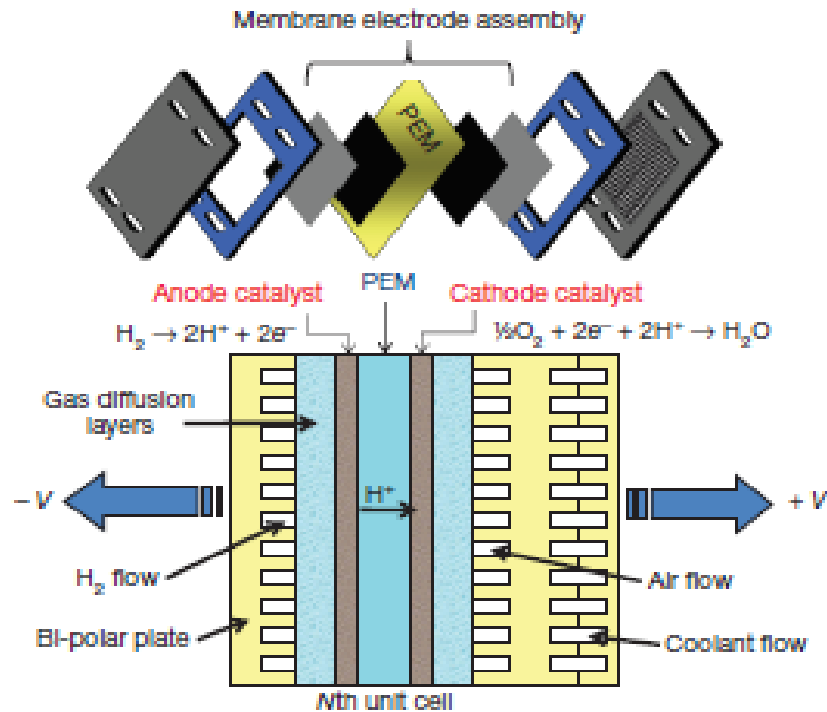


Figure 1- 3 Fuel cell components, Nth unit cell in a fuel cell stack, showing expanded MEA.

1.5 Challenges for the commercialization of PEMFC

The major challenges associated with the commercialization of PEMFC are the durability and the cost of electrocatalyst (Pt-based). The minimum life time requirement for stationary application is 40,000 h and 5,000 h in case of automotive (as per fixed by United States Department of Energy). The problem of durability is raised due to MEA contamination and water management system which lead to Pt accumulation, MEA degradation and carbon erosion. [14] The ORR kinetics is almost six times slower than that of HOR which limits the overall performance, so presently the researchers focus is to improve the ORR kinetics by developing cost effective and durable cathode catalyst and electrode. Currently most of the MEA electrocatalysts are Pt-based (metal nanoparticles supported on carbon black), so the major part of cost is due to this scarce precious metal. According to the DOE'S study 2007, the 56% of the total cost is because of Pt/C catalyst used in PEM fuel cell. The only way to reduce the cost is to minimize the use of Pt metal or replace it with other metal with highly efficient ORR kinetics. United States Department of Energy (DOE) 2017 targets for Pt loading of less than $0.1 \text{ mg Pt cm}^{-2}$. [10]

Summary:

Carbon fuels are adversely affecting the climate, so the need of time is to find some clean and efficient energy resources. Fuel cell are the energy conversion devices, it converts chemical energy of fuels like hydrogen or methanol directly into chemical energy. Polymer electrolyte membrane fuel cell (PEMFC) is the most common type of fuel cell, in PEMFC hydrogen gets oxidize at anode and the reduction of oxygen at cathode to form water. Recently, there are lot of efforts are being made to improve oxygen reduction reaction because it six times slower than hydrogen oxidation reaction. Pt/C is used as electrocatalyst in PEMFC, but its cost and durability restricts the commercialization of PEMFC. Cost factor can be reduced by reducing the Pt percentage, and the durability issue can be resolved by developing some novel electrocatalysts. US Department of Energy (DOE) 2017 targets for Pt loading of less than 0.1mg Pt cm^{-2} .

References

- [1] M. M. Ra, S. Rehman, and S. Asia, “National energy scenario of Pakistan – Current status , future alternatives , and institutional infrastructure : An overview,” vol. 69, no. October 2016, pp. 156–167, 2017.
- [2] “PDF Renewable Energy Sources and Climate Change Mitigation by O. Edenhofer, R. Pichs-Madruga, Y. Science & Nature Books.” [Online]. Available: <https://secretswomen.me/book/922011132/download-renewable-energy-sources-and-climate-change-mitigation-by-o-edenhofer-r-pichs-madruga-y-.pdf>. [Accessed: 13-Apr-2019].
- [3] Mitra, Manu. (2019). A Study on Advances in Hydrogen Fuel Cells. 1. 1-4. 10.5281/zenodo.2616442.
- [4] “Save the Date: DOE’s 2019 Hydrogen and Fuel Cells Program AMR Department of Energy.” [Online]. Available: <https://www.energy.gov/eere/fuelcells/articles/save-date-doe-s-2019-hydrogen-and-fuel-cells-program-amr>. [Accessed: 13-Apr-2019].
- [5] Y. Wang, K. S. Chen, J. Mishler, S. C. Cho, and X. C. Adroher, “A review of polymer electrolyte membrane fuel cells: Technology, applications, and needs on fundamental research,” *Appl. Energy*, vol. 88, no. 4, pp. 981–1007, 2011.
- [6] K. Schmidt-Rohr, “Why Combustions Are Always Exothermic, Yielding About 418 kJ per Mole of O₂,” *J. Chem. Educ.*, vol. 92, no. 12, pp. 2094–2099, Dec. 2015.
- [7] S. M. J. Zaidi and M. A. Rauf, “Fuel Cell Fundamentals,” in *Polymer Membranes for Fuel Cells*, Boston, MA: Springer US, 2008, pp. 1–6.
- [8] “Types of Fuel Cells | Department of Energy.” [Online]. Available: <https://www.energy.gov/eere/fuelcells/types-fuel-cells>. [Accessed: 13-Apr-2019].
- [9] G. Hoogers, *Fuel cell technology handbook*. CRC Press, pp. 7-15, 2003.
- [10] M. K. Debe, “Electrocatalyst approaches and challenges for automotive fuel cells,” *Nature*, vol. 486, no. 7401, pp. 43–51, 2012.

- [11] “Proton-Exchange Membrane Fuel Cells - an overview | ScienceDirect Topics.” [Online]. Available: <https://www.sciencedirect.com/topics/engineering/proton-exchange-membrane-fuel-cells>. [Accessed: 13-Apr-2019].
- [12] R. S. Khurmi and R. S. Sedha, *Material science*. S. Chand, pp, 25-29, 2005.
- [13] M. Kiani *et al.*, “Recent developments in electrocatalysts and future prospects for oxygen reduction reaction in polymer electrolyte membrane fuel cells,” *J. Energy Chem.*, vol. 27, no. 4, pp. 1124–1139, 2018.
- [14] D. Candusso, D. Hissel, A. Hernandez, and A. Aslanides, “A review on PEM voltage degradation associated with water management : Impacts , influent factors and characterization,” vol. 183, pp. 260–274, 2008.

Chapter 2 Literature Review

2.1 Recent developments in oxygen reduction reaction

From the last few decades, a lot of efforts were being done to reduce the Pt loading. The Pt loading has been reduced to 0.4 mg cm^{-2} . Although the Pt loading has been reduced reasonably but the Pt price also increased in this period which somehow balanced all the efforts. So, the approach to reduce the Pt loading was not that much effective. The second approach of using non-noble metal electrocatalyst seems attractive. This approach has been appreciated widely for the commercialization of PEM fuel cell [1]. Unfortunately, the highest performance non-noble metal catalyst (e.g., Fe and Co based supported on carbon) are still lagging behind the commercial Pt/C in terms of performance and durability. Out of all the non-noble metal electrocatalyst the carbon supported nitrogen doped non-noble metal catalyst nanocomposites are the most feasible electrocatalyst for ORR. These M-N_x/C nanocomposites (whereas M= Fe, Co, Cu, Ni etc.) are prepared by the pyrolysis of metal, nitrogen carbon precursors [2,3].

As the non-noble metals have reasonably low cost as compared to Pt/C, the increased loading is not a problem unless the catalyst layer thickness approaches to 100 μm , after than the mass transport problem comes into play [4]. Electrochemical performance does not only take in to account the ORR performance but it also includes the mass transport, chemical and structural aspects and electronic transport as well [5]. Despite of all the developments in the field of non-noble metal electrocatalyst for ORR, still the stability and catalytic activity have not been reached to the desired performance.

2.2 Introduction to Oxygen Reduction Reaction

2.2.1 Electrochemical Oxygen Reduction Reaction

As mentioned in the previous chapter 1, the performance of the fuel cell is limited due ORR kinetics, so the sluggish ORR kinetics is major reason for the ongoing research. The redox potential of ORR at 25°C is 1.229V for 4-electrons pathway [6]. For high performance Pt electrocatalyst, the ORR onset potential is 1V which is 229mV less than the thermodynamic onset potential. The low density of catalytic defect sites on Pt surface and sluggish ORR kinetics are the reasons for lower onset potential of Pt electrocatalyst.

So, the understanding of ORR mechanism is crucial for the development of efficient and effective ORR electrocatalyst.

The ORR is not a simple process, there are a number of intermediates involve in this process, ORR kinetics is dependent on many experimental factors like type of electrode and electrolyte. There are two pathways in which this reaction could take place either its 4-electrons pathway or its 2-electrons pathway in aqueous electrolyte [7].

In aqueous acidic media:

a) 4-electrons pathway



b) 2-electrons pathway



In aqueous alkaline media:

a) 4-electrons pathway



b) 2-electrons pathway



In the PEMFC the 4-electrons pathway is preferred as it's a single step ORR [8].

2.2.2 ORR Mechanism

The ORR mechanism has been studied in a number of reviews. ORR follows different mechanisms due to different types of electrode materials and their physicochemical properties such as crystal structure, porosity, grain size, etc. The steps involved in an ORR: O₂ adsorption, charge transfer, O-O bond breakage, and desorption. In this study the mechanism of ORR on the metal electrode will be discussed.

2.2.3 ORR mechanism on Pt-electrode

So far, Pt is still considered as the most efficient electrocatalyst for this reaction in acidic as well as in basic media, Pt catalysed ORR has been extensively studied. On Pt electrode the ORR takes place through a 4-electron transfer pathway. The high performance of Pt can be justified due to its unique crystal geometry (Pt-Pt bonding) and its d-band electronic structure.

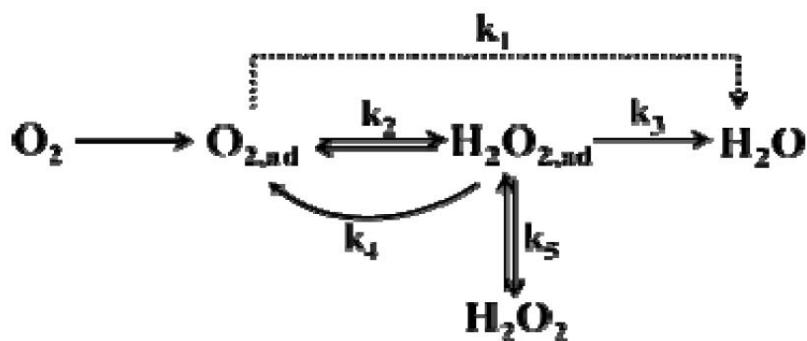


Figure 2- 1 Schematic illustration of ORR kinetics

The ORR mechanism on Pt electrode is shown in Figure 2-1, the O₂ can be reduced to water directly in a single step at a rate constant of k_1 , without the formation of any intermediates (4-electron pathway for ORR), or it can be reduced by a series of 2-electron pathways: first the reduction of O₂ into H₂O₂ at a rate constant of k_2 and then H₂O₂ is reduced to water at k_3 rate constant. H₂O₂ could be decomposed to O₂ at k_4 rate constant or desorbed from the electrode surface with a rate of k_5 . Before all these processes, O₂ needs to be dissociated into O₂²⁻ to transfer the first electron. Oxygen has the dissociation energy

of $498.3 \text{ kJ mol}^{-1}$, this high dissociation energy implies that this dissociation could only be favourable when the M-O bond (M is for metal) is very strong, ($>250 \text{ kJ mol}^{-1}$). On the other hand, metals with stronger M-O bond also have very strong M-OH bond which is highly unfavourable for ORR. So, the ORR kinetics is very complex, and it depends on many other factors, such as the size of Pt particles, anions in the electrolyte, crystal structure, etc.

2.2.4 ORR mechanism on precious metal electrodes

The ORR performance of precious metal electrode has also been very widely studied, but all these metals show relatively lower catalytic activity than Pt and they are not very stable in the electrochemical ORR environment. A comprehensive study was done by Nørskov *et al.* on the activity of metal electrocatalyst for ORR, in this study oxygen binding energy and hydroxyl binding energy with different metals were compared and found that Pt metal has the highest activity for ORR as Pt has the smallest value for the ratio M-OH bond energy to M-O bond energy. The catalytic activity of precious metal on the basis of M-OH and M-O bond strengths ratio has shown in Figure 2-2.

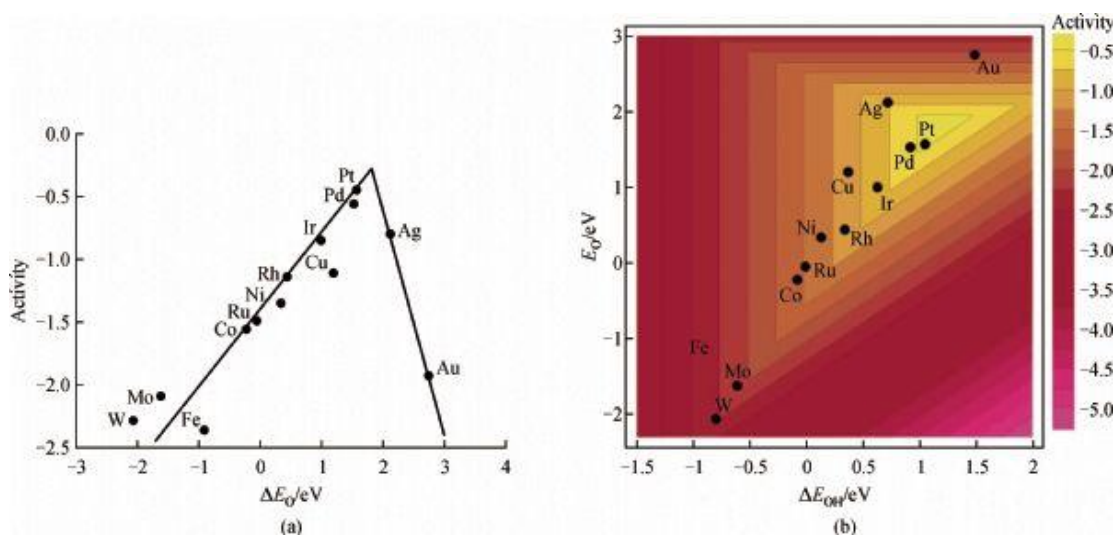


Figure 2- 2 Plot of ORR activity as function of M-O binding energy (a) and M-OH binding energies (b)

The above study shows that Pt has the highest activity, and it has shown the best electrocatalytic performance for ORR. The scarcity of Pt metal results in its high cost and the second issue with Pt-based electrocatalyst is the stability. So, there is a lot of research is been done to reduce the amount of platinum or to replace the platinum with other non-noble and abundant metal catalyst. There are examples available in literature which show that alloying of platinum with other metals (Co, Ni, Fe, Cu) exhibit better catalytic performance than commercial Pt/C. Pd-based and non-noble metal based catalyst has also been used as the substitute for Pt.

Figure 2-2 shows that Cu has higher activity for ORR than other non-noble metals. Although the Cu-based electrocatalysts have not shown the better performance than commercial Pt/C catalyst, but there are a number of experimental and theoretical studies which show the potential of Cu-based electrocatalyst for ORR [9].

2.3 Metal Organic Frameworks and electrocatalysis

Metal organic frameworks (MOFs) are advanced materials which have become very popular in the recent years because of their fascinating structural and morphological properties. [10] MOFs are defined as a class for materials in which organic polyfunctional ligand (commonly 1,4-benzenedicarboxylic acid and 1,3,5-benzene-tricarboxylic acid) is used to form a coordination porous networking structures with specific transition metal.[11] Due to the unique properties of MOFs, they are used for storage, separation and purification of gases, [12,13] also for heterogeneous catalysis, [14,15] drug release [16] and sensing [17].

Several techniques have been used for the synthesis of MOFs. The most commonly use methods are the solvothermal synthesis and synthesis at room temperature [18]. In solvothermal synthesis the mixture of organic linker and metal salt is heated in a solvent system which is contains N,N-dimethylformamide functional group. While in the room temperature synthesis the starting materials (organic linker and metal salt) is mixed together in a solution at ambient temperature , for the initiation of reaction the mixing is done in the presence of triethylamine which deprotonate the organic linker to precipitate the MOFs [19]. Table. 2-1 represents the different types of MOFs along with the linkers used [20].

Maryam Jahan et.al investigated the Cu-MOF composite with graphene oxide (GO) and found that this composite shows excellent ORR performance. In PEM fuel cell it showed power density of 76% of commercial Pt/C [21].

MOFs have used as template to fabricate nanostructured carbon materials [22]. Hetroatoms (e.g., B, S, N and P) precursor is combined with MOF to enhance the electrocatalytic activity of composite. Rui Wang et al. prepared a Cu-MOF based electrocatalyst with N and P doping which has shown excellent activity for both ORR and hydrogen evolution reaction (HER) [23].

Carbon supported Pt-M alloy electrocatalyst have been used developed, and have shown better ORR performance than commercial Pt/C (M= Fe, Co, Ni, Cu, etc.). Pt:M of 3:1 has 2-3 times higher activity than state of the art commercial Pt/C catalyst. Strasser et al prepared a Pt-Cu alloy catalyst with very low percentage of Pt (Cu:Pt ration of 3:1) and then by electrochemical voltage cycling removed almost 90% of Cu and enhanced the catalyst activity 4-6 folds than that of commercial Pt/C [24].

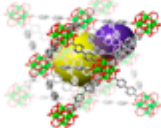
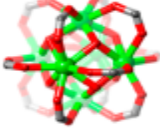
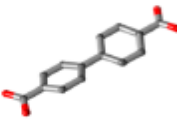
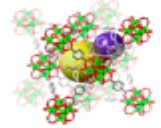
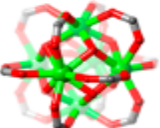
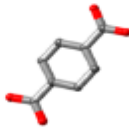
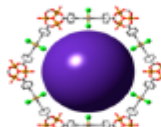
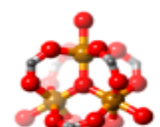
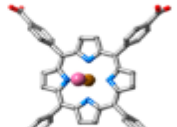
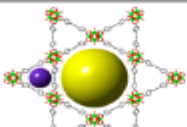
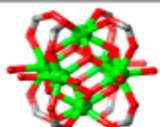
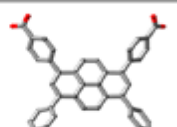
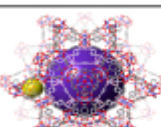
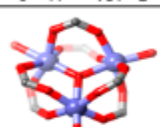
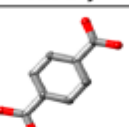
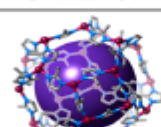
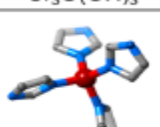
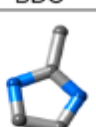
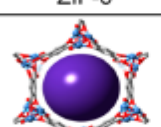
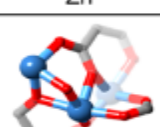
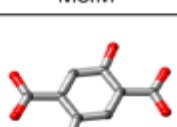
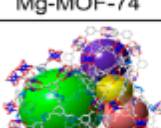
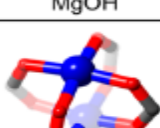

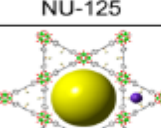
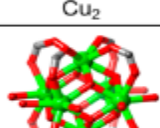
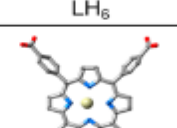
MOF	Metal Node	Organic Linker
 UiO-67	 $Zr_6O_4(OH)_4$	 BPDC
 UiO-66	 $Zr_6O_4(OH)_4$	 BDC
 PCN-600(M)	 $Fe_3O(OH)_3$	 M-TCPP
 NU-1000	 $Zr_6O_4(OH)_8(H_2O)_4$	 TBAPy
 Cr-MIL-101	 $Cr_3O(OH)_3$	 BDC
 ZIF-8	 Zn	 MelM
 Mg-MOF-74	 MgOH	 $BDC-(OH)_2$
 NU-125	 Cu_2	 LH ₆
 PCN-222(Fe)	 $Zr_6O_4(OH)_8(H_2O)_4$	 Fe-TCPP

Table 2-1 Structures of MOFs according to the organic linker used

Summary:

So far the Pt amount in PEMFC has been reduced to 0.4 mg Pt/cm² but still it is not up to the DOE 2017 target. Non-noble metal electrocatalysts are being popular especially Cu, Co, Fe and Ni have shown a comparative ORR activity, these metals are still not competing with Pt. The ORR can take place in two reaction mechanisms, 4e⁻ and 2e⁻ mechanism, for ORR 4e⁻ is preferable. Metal organic frameworks (MOFs) are advanced materials with very high surface area which is desirable for catalysis. MOFs are usually not good conductors but still they are being used as electrocatalyst with some modification in their structure and composition. Cu MOF composite with graphene have shown very high ORR activity. Similarly the pyrolysis of zif-67 yield an excellent ORR catalyst which contains carbon nanotubes. Non-noble metal alloy with Pt also have shown a reasonably good ORR activity with no durability issues. The objective of the study was to develop an excellent ORR catalyst with minimum Pt loading.

References

- [1] M. Kiani *et al.*, “Recent developments in electrocatalysts and future prospects for oxygen reduction reaction in polymer electrolyte membrane fuel cells,” *J. Energy Chem.*, vol. 27, no. 4, pp. 1124–1139, 2018.
- [2] C. W. B. Bezerra *et al.*, “Review article A review of Fe – N / C and Co – N / C catalysts for the oxygen reduction reaction,” vol. 53, pp. 4937–4951, 2008.
- [3] A. Ishihara, Y. Ohgi, K. Matsuzawa, S. Mitsushima, and K. Ota, “Electrochimica Acta Progress in non-precious metal oxide-based cathode for polymer electrolyte fuel cells,” vol. 55, pp. 8005–8012, 2010.
- [4] E. Antolini and E. R. Gonzalez, “Applied Catalysis B : Environmental Tungsten-based materials for fuel cell applications,” *Applied Catal. B, Environ.*, vol. 96, no. 3–4, pp. 245–266, 2010.
- [5] I. Dumitrescu and R. M. Crooks, “Effect of mass transfer on the oxygen reduction reaction catalyzed by platinum dendrimer encapsulated nanoparticles,” *Proc. Natl. Acad. Sci. U. S. A.*, vol. 109, no. 29, pp. 11493–7, Jul. 2012.
- [6] J. Zhang, Ed., *PEM Fuel Cell Electrocatalysts and Catalyst Layers*. London: Springer London, pp. 90-97, 2008.
- [7] “Oxygen Reduction Reaction,” 2016.
<http://www.rsc.org/suppdata/c6/ra/c6ra23100d/c6ra23100d1.pdf>
- [8] O. T. Holton and J. W. Stevenson, “The Role of Platinum in Proton Exchange Membrane Fuel Cells,” *Platin. Met. Rev.*, vol. 57, no. 4, pp. 259–271, Oct. 2013.
- [9] C. Du, X. Gao, and W. Chen, “Recent developments in copper - based , non - noble metal electrocatalysts for the oxygen reduction reaction,” *Chinese J. Catal.*, vol. 37, no. 7, pp. 1049–1061, 2016.
- [10] E. D. Dikio and A. M. Farah, “Synthesis , Characterization and Comparative Study of Copper and Zinc Metal Organic Frameworks,” vol. 2, no. 4, pp. 1386–1394, 2013.
- [11] C. G. Carson *et al.*, “Synthesis and Structure Characterization of Copper Terephthalate Metal – Organic Frameworks,” pp. 2338–2343, 2009.
- [12] R. Banerjee *et al.*, “High-throughput synthesis of zeolitic imidazolate frameworks and application to CO₂ capture,” *Science*, vol. 319, no. 5865, pp. 939–43, Feb. 2008.
- [13] K. Sumida *et al.*, “Hydrogen storage and carbon dioxide capture in an iron-based sodalite-type metal – organic framework (Fe-BTT) discovered via high-throughput methods †,” pp. 184–191, 2010.
- [14] J. Lee, O. K. Farha, J. Roberts, K. A. Scheidt, S. T. Nguyen, and J. T. Hupp, “2009 Metal – organic frameworks issue Metal – organic framework materials as catalysts w,” no. 5, 2009.

- [15] D. M. Robinson *et al.*, “Photochemical Water Oxidation by Crystalline Polymorphs of Manganese Oxides: Structural Requirements for Catalysis,” 2013.
- [16] A. C. Mckinlay *et al.*, “Minireviews BioMOFs : Metal – Organic Frameworks for Biological and Medical Applications,” pp. 6260–6266, 2010.
- [17] K. Sumida *et al.*, “Carbon Dioxide Capture in Metal–Organic Frameworks,” *Chem. Rev.*, vol. 112, no. 2, pp. 724–781, Feb. 2012.
- [18] P. Pachfule, R. Das, P. Poddar, and R. Banerjee, “Solvothermal Synthesis, Structure, and Properties of Metal Organic Framework Isomers Derived from a Partially Fluorinated Link,” *Cryst. Growth Des.*, vol. 11, no. 4, pp. 1215–1222, Apr. 2011.
- [19] Y. Sun and H.-C. Zhou, “Recent progress in the synthesis of metal–organic frameworks,” *Sci. Technol. Adv. Mater.*, vol. 16, no. 5, p. 054202, Oct. 2015.
- [20] A. J. Howarth, A. W. Peters, N. A. Vermeulen, T. C. Wang, J. T. Hupp, and O. K. Farha, “Best Practices for the Synthesis, Activation, and Characterization of Metal – Organic Frameworks,” 2017.
- [21] M. Jahan, Z. Liu, and K. P. Loh, “FULL PAPER A Graphene Oxide and Copper-Centered Metal Organic Framework Composite as a Tri-Functional Catalyst for HER ,” pp. 5363–5372, 2013.
- [22] H. Wang, Q. Zhu, R. Zou, and Q. Xu, “Metal-Organic Frameworks for Energy Applications,” *CHEMPR*, vol. 2, no. 1, pp. 52–80, 2017.
- [23] R. Wang, X. Dong, J. Du, J. Zhao, and S. Zang, “MOF-Derived Bifunctional Cu₃P Nanoparticles Coated by a N , P-Codoped Carbon Shell for Hydrogen Evolution and Oxygen Reduction,” vol. 1703711, pp. 1–10, 2018.
- [24] Z. Yu, J. Zhang, Z. Liu, J. M. Ziegelbauer, and H. Xin, “Comparison between Dealloyed PtCo₃ and PtCu₃ Cathode Catalysts for Proton Exchange Membrane Fuel Cells,” 2012.

Chapter 3 Characterization

Characterization is the process by which the structural properties of the materials are determined using different techniques, including SEM, XRD, XPS, and TEM etc. The other type of characterization is application specific in this study the electrochemical characterization is done for oxygen reduction reaction for this potentiostat with three electrode system was used.

3.1 Physical Characterization

3.1.1 Scanning Electron Microscopy (SEM/EDS)

Scanning electron microscopy is an imaging technique that produce scanned images by focusing high beam of electrons on the sample. The electrons interact with the surface of the sample and produce different signals according to the nature of sample. These signals are used to determine the topology and composition of the sample [1].

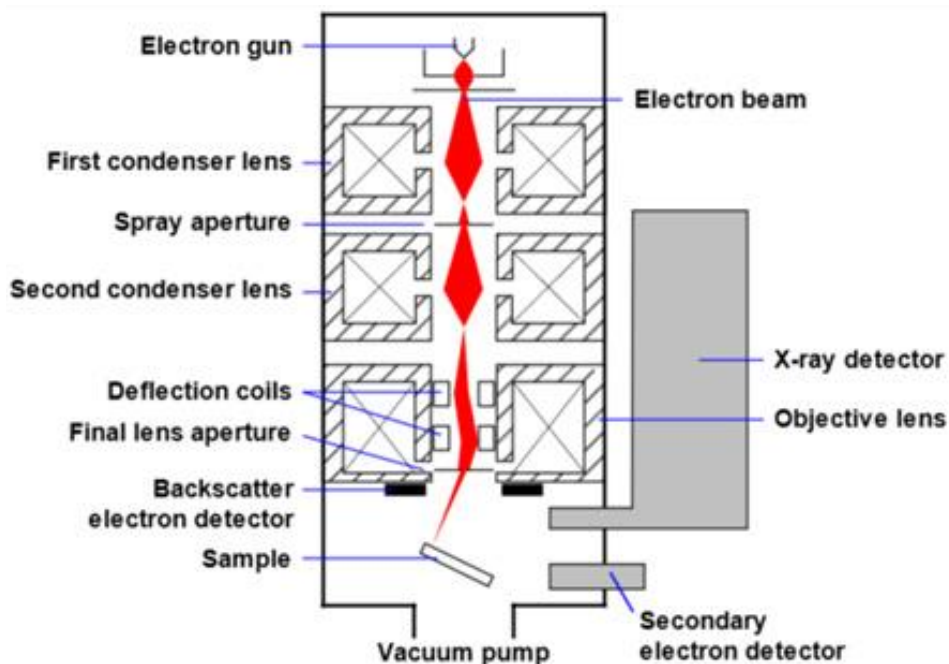


Figure 3- 1 Working principle of SEM

3.1.2 Transmission Electron Microscopy (TEM)

Transmission electron microscopy is a characterization technique in which a high energy electron beam is passed through the sample to produce an image. The image is formed because of the interaction of electrons with the sample. An ultrathin layer of around 100nm is used as specimen for TEM [2].

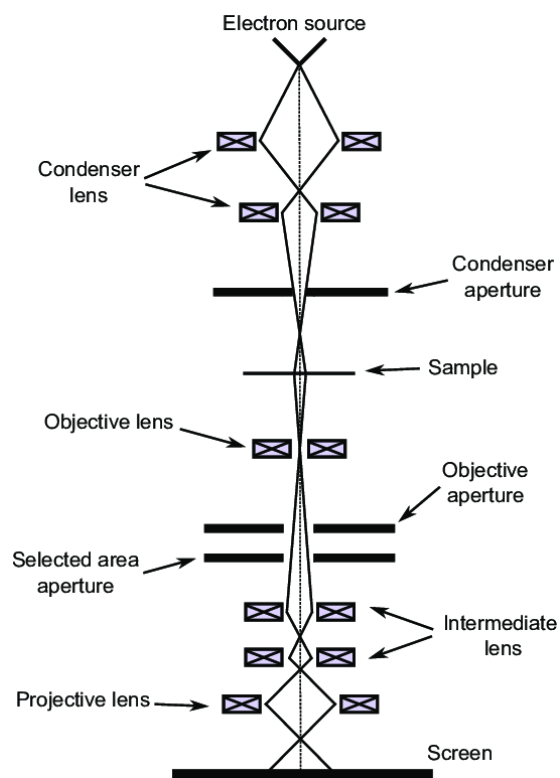


Figure 3- 2 Schematic of TEM

3.1.3 X-ray Photoelectron Spectroscopy (XPS)

X-ray photoelectron spectroscopy is the only versatile technique for surface analysis of materials. It is a surface sensitive non-destructive characterization technique. It gives information about the surface chemical composition and the electronic state of elements present in the material [3].

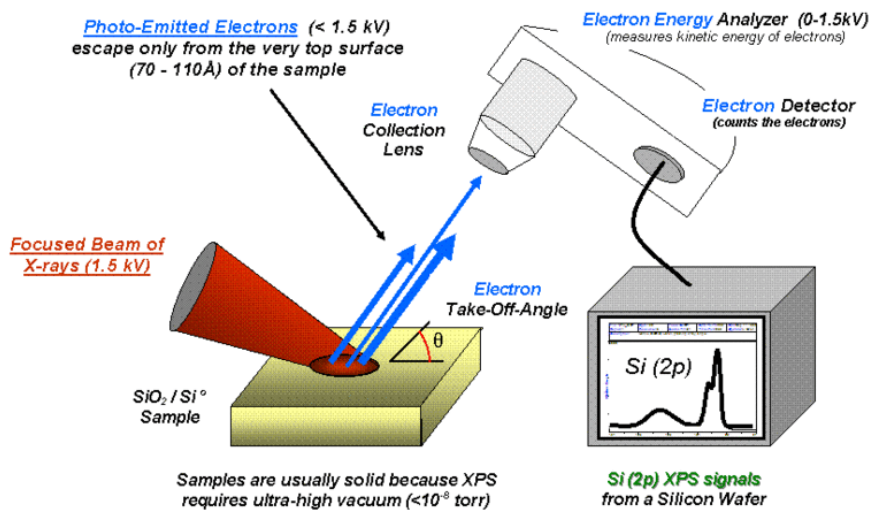


Figure 3- 3 Basics of XPS

3.1.4 X-ray diffraction (XRD)

X-ray diffraction is a non-destructive characterization technique that is used to determine the crystallinity and chemical structure of the metal and metal alloy based materials. X-ray diffraction is basically the elastic scattering of photons due to the atoms in periodic lattice. In phase diffracted x-rays give the constructive interference [4].

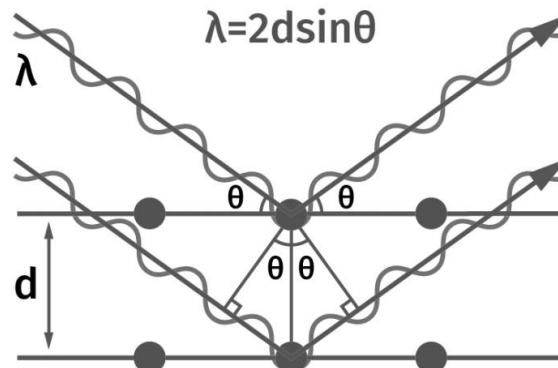


Figure 3- 4 XRD illustration

3.1.5 Thermal Gravimetric Analysis (TGA)

Thermal gravimetric analysis is a technique by which the thermal analysis of the sample is done to measure the physical and chemical changes. These changes are measured as the function of temperature (constant heat rate) and time [5].

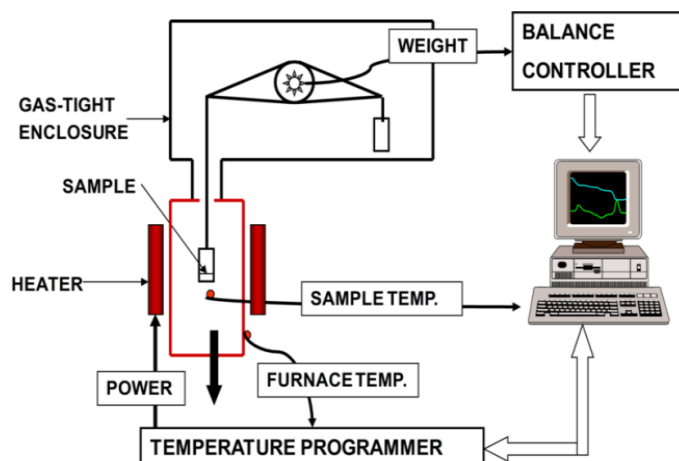


Figure 3- 5 Components of TGA

3.1.6 Fourier Transform Infrared Spectroscopy (FTIR)

Fourier transform infrared spectroscopy is a technique which is used to determine the types of bond formation within the structure of a material. An infrared spectrum represents the frequency of vibrations due to different kinds of bonds between the atoms making up the material. FTIR can also be used to determine the chemical composition of sample [6].

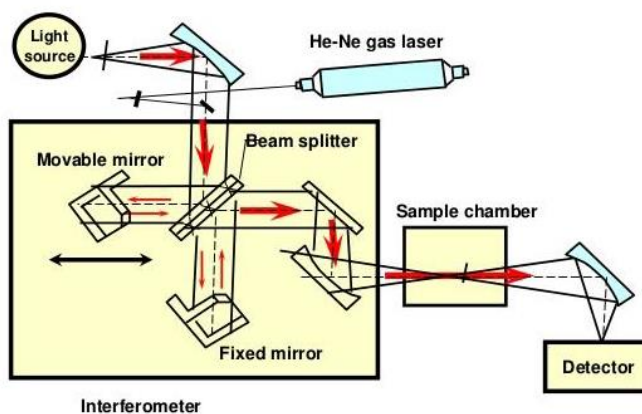


Figure 3- 6 Working principle of FTIR

3.2 Electrochemical Characterization

Electrochemical characterization techniques are used to determine the electrochemical activity of catalysts for different kinds of reactions e.g. oxygen reduction reaction, hydrogen evolution reaction, carbon dioxide reduction.

3.2.1 Cyclic Voltammetry (CV)

Cyclic voltammetry is the most commonly used technique to study the electrochemical properties of materials. It gives information about the kinetics of electrode reactions. In CV is performed by cycling the potential of the working electrode and the resulting current is measured. The potential difference of working electrode is measured against a reference electrode (Ag/AgCl).

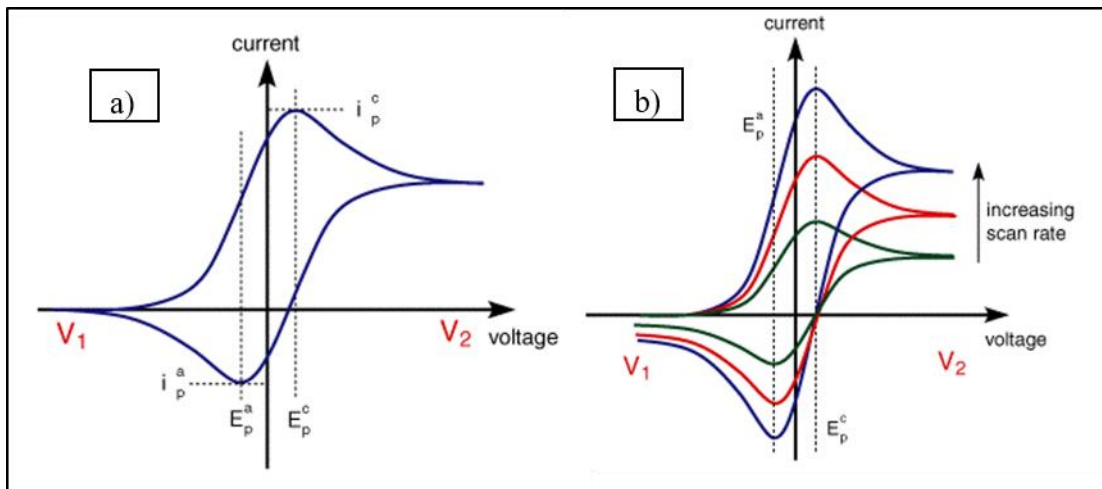


Figure 3- 7 (a) basic CV plot (b) CV plot at multiple scan rates(mV/s)

3.2.2 Linear Sweep Voltammetry (LSV)

In linear sweep voltammetry technique the voltage is sweep between reference and working electrode at constant scan rate. The voltage scanning window is defined by the specific reaction (ORR, OER, HER) and the type of electrocatalyst. In contrast to CV the voltage is swept in only one direction. Voltage is scanned from a lower limit to upper limit as shown in Figure 3-8 [7]. The linear sweep voltammogram slope depends on the electron transfer number, electrochemical activity of the catalyst and voltage scan rate.

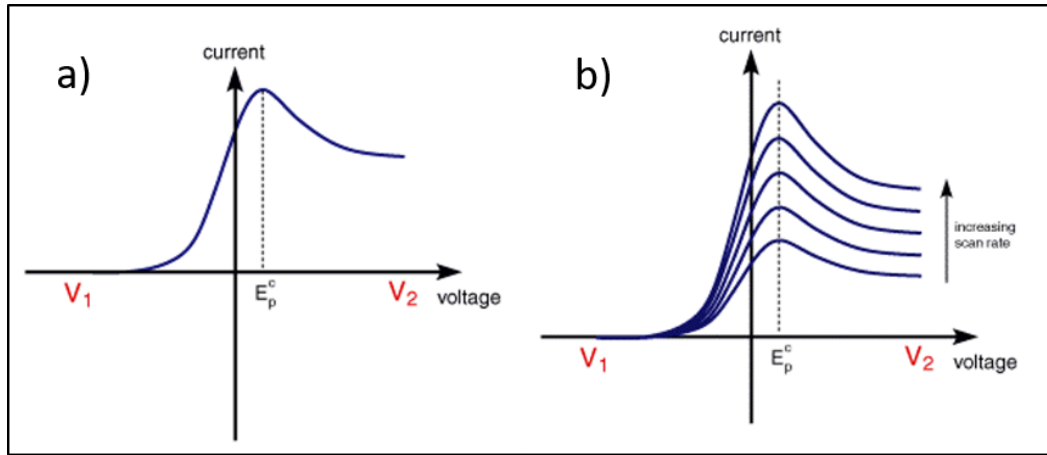


Figure 3- 8 (a) general LSV graph (b) LSV at multiple scan rates (mV/s)

3.2.3 Electrochemical impedance spectroscopy (EIS)

Electrical Impedance spectroscopy (EIS) is a technique to determine the impedance due to the electrocatalyst. It measures the resistance of a circuit with respect to frequency. The losses in fuel cell are categories as ohmic and non-ohmic losses. The ohmic losses are measured by simply using direct current (DC) but on the other hand non-ohmic losses like adsorption on electrode surface and charge transfer t double layer is measured by alternating current at a fixed frequency [8][9]. EIS can also be used to determine the diffusion co-efficient. Nyquist plot is shown for randles circuit in the Figure 3-9, W_{sc} is Warburg impedance which is explained in the reference. [10].

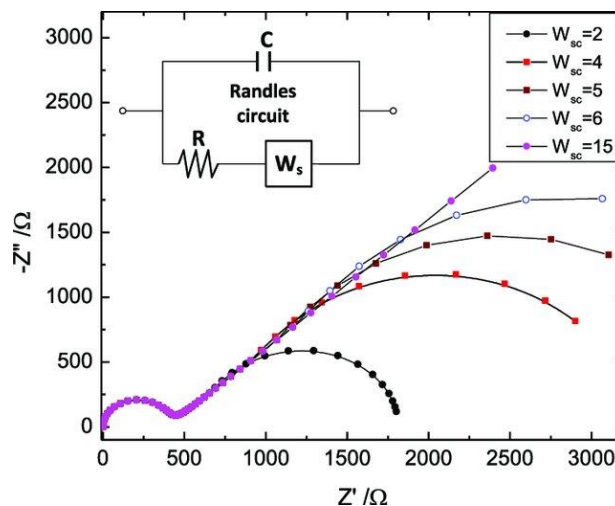


Figure 3- 9 EIS of randles circuit

Summary:

This chapter includes an overview of all the techniques used in the study. SEM and TEM are used for imaging of electrocatalyst to find out the morphology and shape of particles. X-ray is used to determine the crystallographic properties of materials. XPS is done to get into the surface composition. TGA was performed to study thermal analysis and stability. FTIR gives information about the types of bond present in the material. Electrochemical techniques includes CV, LSV and, EIS. CV and LSV provide information about the electrocatalyst activity for specific reaction while EIS tells about the impedance due to working electrode.

References

- [1] L. Reimer, *Scanning Electron Microscopy*, vol. 45. Berlin, Heidelberg: Springer Berlin Heidelberg, pp, 98-105, 1998.
- [2] D. B. Williams and C. B. Carter, “The Transmission Electron Microscope,” in *Transmission Electron Microscopy*, Boston, MA: Springer US, 2009, pp. 3–22.
- [3] P. Van der Heide, *X-ray photoelectron spectroscopy : an introduction to principles and practices*. Wiley-Blackwell, pp, 42-47, 2012.
- [4] C. Suryanarayana and M. G. Norton, “X-Rays and Diffraction,” in *X-Ray Diffraction*, Boston, MA: Springer US, 1998, pp. 3–19.
- [5] “Thermogravimetric Analysis - an overview | ScienceDirect Topics.” [Online]. Available: <https://www.sciencedirect.com/topics/materials-science/thermogravimetric-analysis>. [Accessed: 14-Apr-2019].
- [6] B. Smith, *Fundamentals of Fourier transform infrared spectroscopy*. CRS press, pp, 13-15, 2011.
- [7] “Linear Sweep and Cyclic Voltametry: The Principles — Department of Chemical Engineering and Biotechnology.” [Online]. Available: <https://www.ceb.cam.ac.uk/research/groups/rg-eme/Edu/linear-sweep-and-cyclic-voltametry-the-principles>. [Accessed: 14-Apr-2019].
- [8] M. E. Orazem and B. Tribollet, *Electrochemical impedance spectroscopy*. Wiley, pp, 55-57, 2008.
- [9] E. P. Randviir and C. E. Banks, “Electrochemical impedance spectroscopy: an overview of bioanalytical applications,” *Anal. Methods*, vol. 5, no. 5, p. 1098, Feb. 2013.
- [10] T. Q. Nguyen and C. Breitkopf, “Determination of Diffusion Coefficients Using Impedance Spectroscopy Data,” *J. Electrochem. Soc.*, vol. 165, no. 14, pp. E826–E831, 2018.

Chapter 4 Experimentation

In this chapter all the experimental procedures that are followed in the study are discussed and explained in details along with schematics, including the material synthesis , catalyst ink preparation and electrochemical setup.

4.1 Materials

$\text{Cu}(\text{NO}_3)_2 \cdot 3(\text{H}_2\text{O})$ and terephthalic (tpa) acid was used in the synthesis of Cu-tpa MOF. Chloroplatinic acid H_2PtCl_6 was used for Pt loading. Dimethylformamide (DMF), Ethanol, deionized water (DI) were used as solvents. Other chemical and solvents used were Perchloric acid (HClO_4), acetone, 5 wt% Nafion was purchased from USA. Gases used were Argon (Ar), Oxygen (O_2), Nitrogen (N_2), Hydrogen (H_2).

4.2 Cu-tpa MOF synthesis

Cu-tpa MOF was synthesized by method described in the literature [1]. In a typical synthesis 5mg of $\text{Cu}(\text{NO}_3)_2 \cdot 3\text{H}_2\text{O}$ was dissolved in deionized (DI) water, 2mg of terephthalic acid was dissolved in mixed solution of 40ml N,N-dimethyl formaldehyde (DMF) and 40ml of ethanol. Both the above mentioned solutions (containing $\text{Cu}(\text{NO}_3)_2 \cdot 3\text{H}_2\text{O}$ and terephthalic acid) were mixed together and placed on hot plate at 80°C for 24h with continuous stirring. The blue powder was centrifuged and washed with DMF and DI water. The collected powder was dried at 80°C in a vacuum oven.

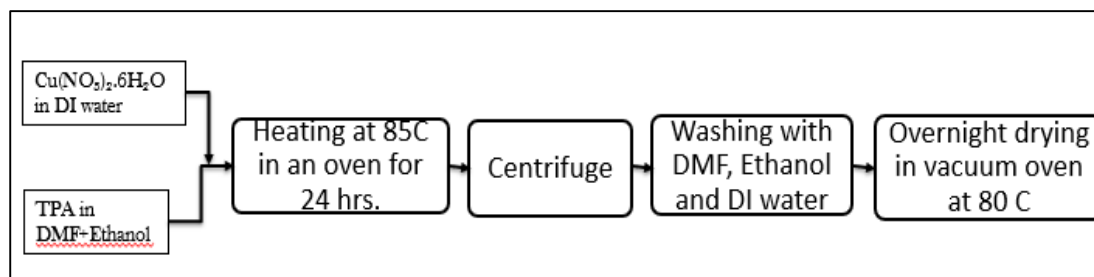


Figure 4- 1 Synthesis of Cu-tpa MOF



Figure 4- 2 Cu-tpa MOF sample

4.3 Synthesis of Cu/NC

100mg of Cu-tpa MOF dried in vacuum oven at 80°C for 2 h. The dried powder was first heated to 350°C and stayed for 1.5 h. Then it was heated to 700°C at the heating rate of 2°C /min and kept at 700°C for about 3.5 h under the constant flow of Ar-H₂ (90% Ar) in the tube furnace. After the natural cooling down of the tube furnace to room temperature the black carbonized powder was collected. Then this collected powder was acid washed and then Cu/NC was recovered after centrifugation, multiple washings with DI water and drying at 80°C in vacuum oven [2].

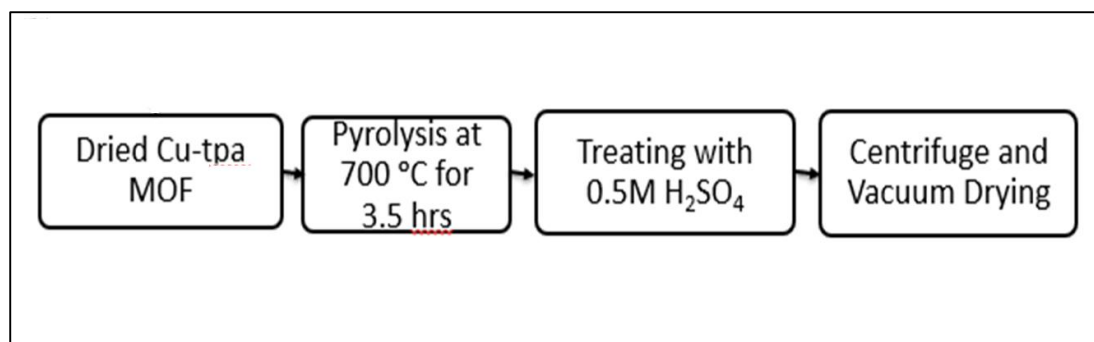


Figure 4- 3 Synthesis of Cu/NC

4.4 Synthesis of CuPt/NC

100mg of Cu-tpa MOF was mixed with 0.1ml of 96.5mM H₂PtCl₆ and the mixture was dried at 80°C for 2 h. The dried powder was heated to 350°C for 1.5 h then heated to 700°C at the ramp rate of 2°C /min and kept it at 700°C for 3.5 h under the constant flow of Ar-H₂ (90% Ar) in the tube furnace. After cooling down the furnace temperature

naturally the black pyrolyzed powder was collected. After the acid wash the resultant catalyst with 10%Pt loading was recovered after centrifugation, multiple washings with DI water and drying at 80°C in vacuum oven [2].

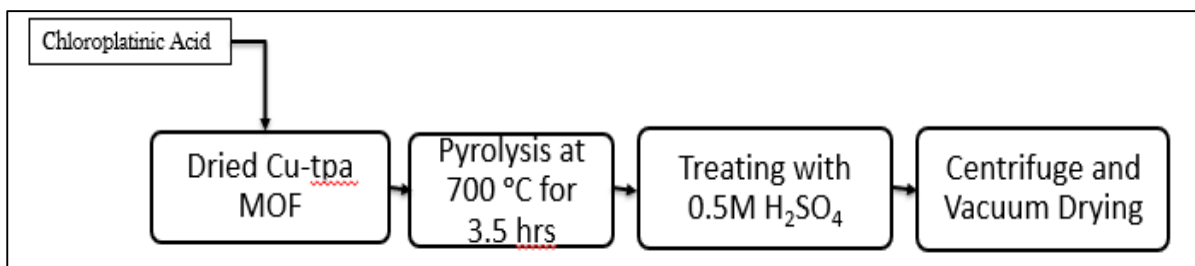


Figure 4- 4 Synthesis of CuPt/NC



Figure 4- 5 CuPt/NC sample

4.5 Catalyst ink

Catalyst ink was prepared by dissolving 2 mg of catalyst (Cu/NC, CuPt/NC and Pt/C) in 1 ml of stock solution and sonicated the suspension in ultrasonic bath for 30 min. Stock solution was prepared by mixing together 7.6 ml of DI water, 2.4 ml of iso-propyl alcohol and 0.1 ml of 5 wt % nafion dispersion [3].

4.6 Electrode preparation

The catalyst electrode film was prepared on glassy carbon by dropping 5-10 ul of ink on it and dried it for 20 min at 700 rpm. The thin films of Commercial CuPt/NC, Pt/C and Cu/NC were deposited on the electrode by the same method.

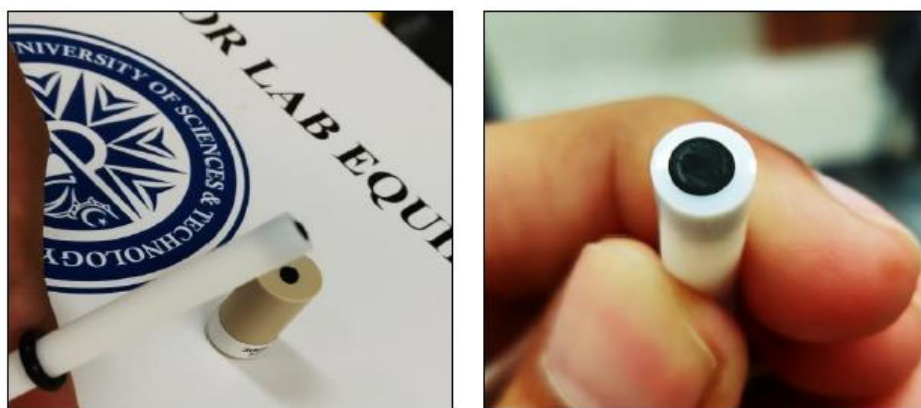


Figure 4- 6 Glassy carbon electrode with ink deposited on it

4.7 Electrochemical setup

Three electrode system was used for electrochemical measurements. CHIE-760 electrochemical workstation was used. Three electrode system consists of working electrode (glassy carbon), reference electrode (Ag/AgCl) and counter electrode (Pt). Electrochemical testing that can be performed using this system are linear sweep voltammetry (LSV), cyclic voltammetry (CV) and, electronic impedance spectroscopy (EIS) [4].

Summary:

This chapter highlights the overall scheme of experimentation. Cu-tpa MOF was prepared by using Cu salt with terephthalic acid (organic linker). After that the pyrolysis of Cu-tpa MOF was done with and without Pt loading. Cu/NC and CuPt/NC ink was prepared for electrochemical testing using nafion. Working electrode was prepared by dropping 5-10 ul of ink on glassy carbon electrode and then dried it. Electrochemical testing system used was three electrode system.

References

- [1] X. Wang *et al.*, “Highly dispersible and stable copper terephthalate MOF-graphene oxide nanocomposite for electrochemical sensing application Highly dispersible and stable copper terephthalate MOF-graphene oxide nanocomposite for electrochemical sensing application,” 2014.
- [2] B. Y. Xia, Y. Yan, N. Li, H. Bin Wu, X. W. D. Lou, and X. Wang, “A metal-organic framework-derived bifunctional oxygen electrocatalyst,” *Nat. Energy*, vol. 1, no. 1, pp. 1–8, 2016.
- [3] K. Shinozaki, J. W. Zack, R. M. Richards, B. S. Pivovar, and S. S. Kocha, “Oxygen Reduction Reaction Measurements on Platinum Electrocatalysts Utilizing Rotating Disk Electrode Technique I . Impact of Impurities , Measurement Protocols and Applied Corrections,” vol. 162, no. 10, pp. 1144–1158, 2015.
- [4] C. G. Zoski, *Handbook of electrochemistry*. Elsevier, pp, 75-89, 2007.

Chapter 5 Results and discussion

5.1 Scanning electron microscopy (SEM) analysis of CuPt/NC

Figure 5-1 shows the SEM images of Cu-tpa MOF before and after pyrolysis. The Cu-tpa MOF particle size is around 400nm. After the pyrolysis the sample was changed into a black powder because of the carbonization of organic linker. The breakdown of unstable organic groups led to the formation of nano-porous carbon on Cu-tpa MOF surface as shown in Figure 5-1 b,c without and with Pt loading respectively. The nano-porous carbon surrounded the Cu and Pt metals. After pyrolysis due to nano-porous carbon the surface of Cu-tpa became uneven and the surface of CuPt/NC is rougher than that of Cu/NC [1].

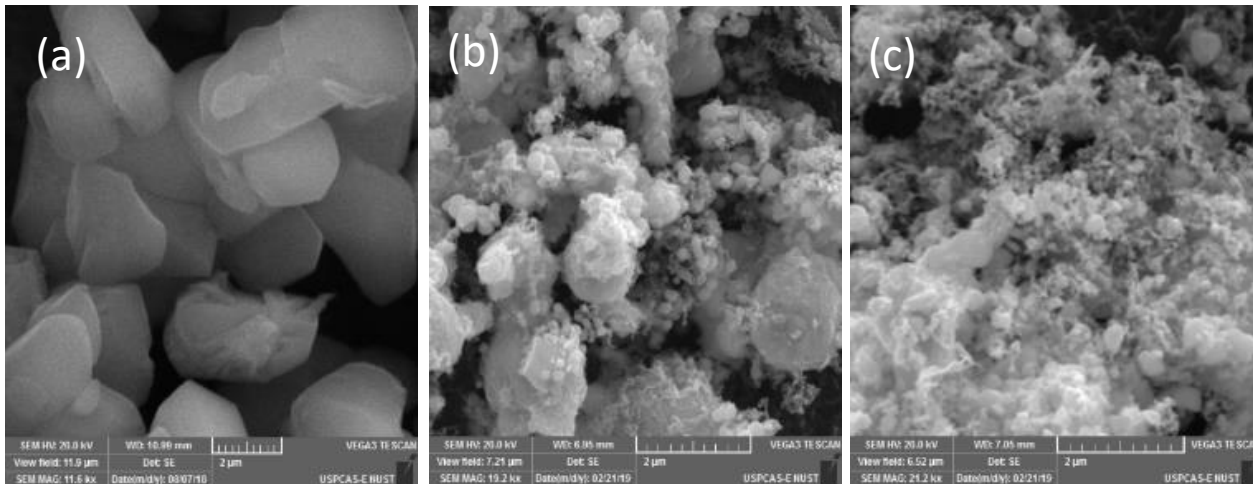


Figure 5- 1 Scanning electron microscopy images of (a) Cu-tpa MOF (b) Cu/NC (c) CuPt/NC

5.2 Transmission electron microscopy (TEM) analysis of CuPt/NC

In Figure 5-2 TEM images of CuPt/NC have shown at three different magnifications of (50nm, 20nm, 10nm), the TEM images indicates that the pyrolyzed sample contains numerous small CuPt NP distributed uniformly on carbon matrix and also Figure 5-2c shows graphitic lattice fringes. The average CuPt nanoparticle is 5nm in size [2].

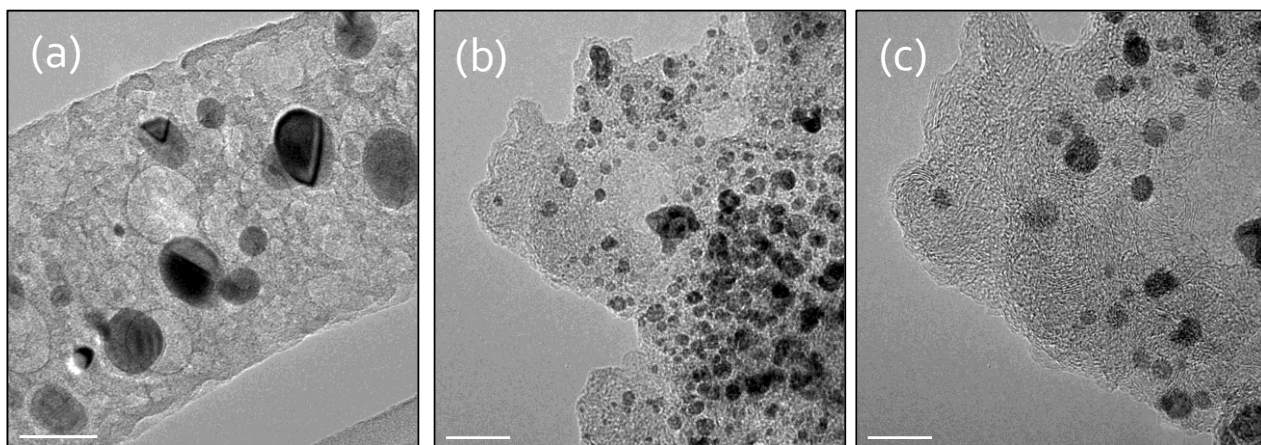


Figure 5- 2 Transmission electron micrographs for CuPt/NC (a) 50nm (b) 20nm (c) 10nm

5.3 X-ray diffraction (XRD) analysis of CuPt/NC

The XRD graph of CuPt/NC shows sharp peak of Cu (111) at 50.7° and Cu (200) at 59.2° (Figure 5-3). A little hump between $20\text{-}30^\circ$ indicates nano-porous carbon. Because of low percentage of Pt very little peak of Pt was observed at 2-theta of 80.3° .

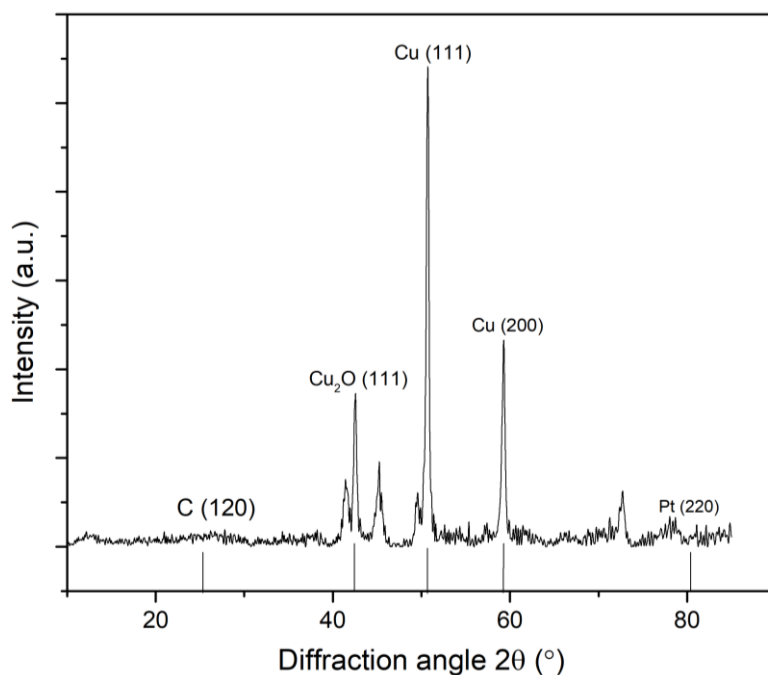


Figure 5- 3 XRD pattern of CuPt/NC

5.4 X-ray photoelectron spectroscopy (XPS) analysis of CuPt/NC

Furthermore the XPS confirms the presence of Pt. A positive electronic shift of 1.45eV (72.45-71eV) and 0.46eV (933-933.46eV) in Pt (4f) and Cu (2p) respectively confirms the alloy formation of CuPt. C (1s) peak at ~286eV and O (1s) peak at 530.8eV attribute to C-O-C and C-O components respectively (Figure 5-4) [3].

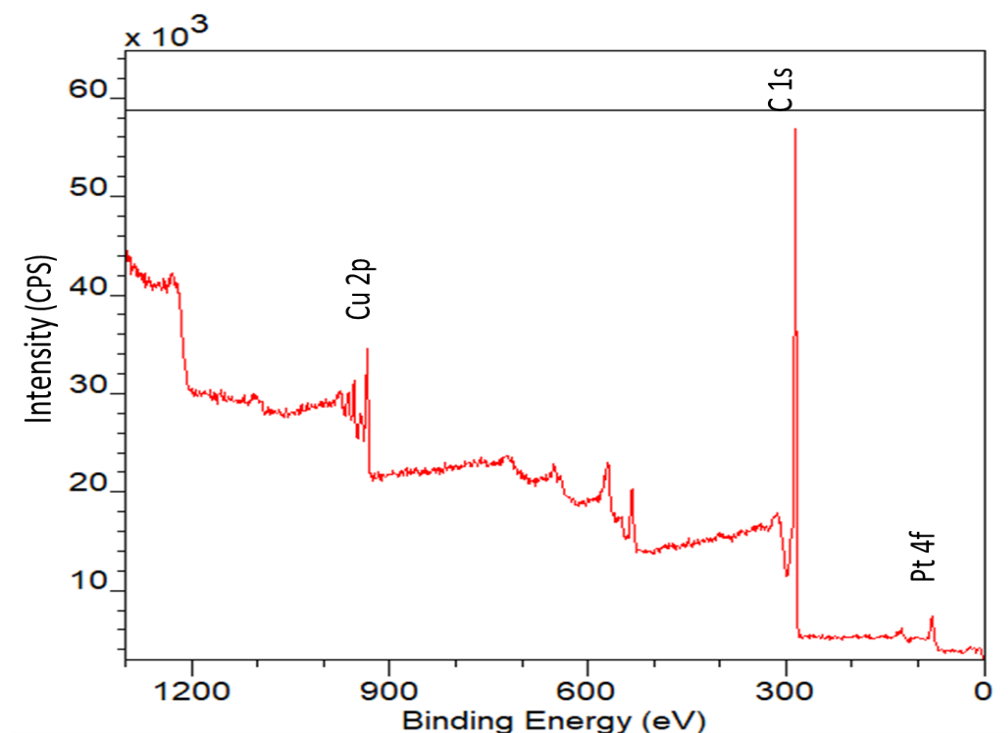


Figure 5- 4 XPS spectrum of CuPt/NC

5.5 Electrochemical testing of CuPt/NC for ORR

Commercial Pt/C is set as benchmarked for CuPt/NC. The CV graphs in Figure 5-5 show that CuPt/NC has the higher ORR activity of than that of commercial Pt/C in 0.1M HClO₄ with oxygen saturation at scanning rate of 50mV/s. The onset and half wave potential for CuPt/NC is observed as 0.9 (vs. RHE) and 0.79V (vs. RHE) respectively

which is better than commercial Pt/C. The ORR dip of CuPt/NC is bigger than that of commercial Pt/C at 0.7V (vs. RHE) as shown in Figure 5-6.

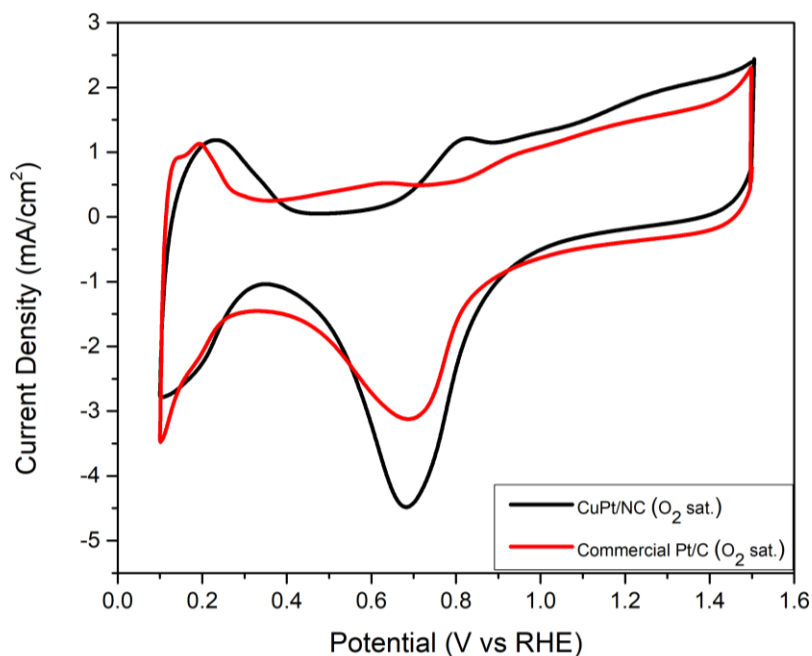


Figure 5- 5 CV plots for CuPt/NC and commercial Pt/C

Figure. 5-6 shows the CV plots of CuPt/NC with oxygen and nitrogen saturation, as the peak for nitrogen is very low but for oxygen a sharp peak is observed at 0.7V (vs. RHE) which confirms ORR activity of CuPt/NC [4].

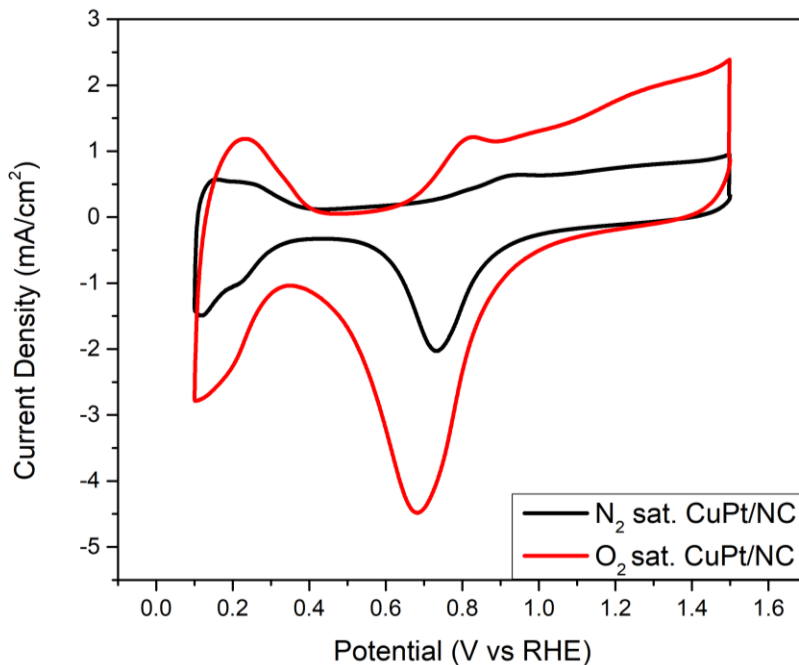


Figure 5- 6 CV plot for CuPt/NC with O₂ and N₂ saturation

Linear sweep voltammetry (LSV) was performed with a rotating disk electrode assembly. LSV measurements of CuPt/NC are made at different rotations (400, 800, 1200, 1600 rpm), in 0.1M HClO₄ with O₂ saturation at scanning rate of 30mV/s. The maximum value limiting current density was recorded as 4 mA/cm² at 1600rpm (Figure 5-7) [5].

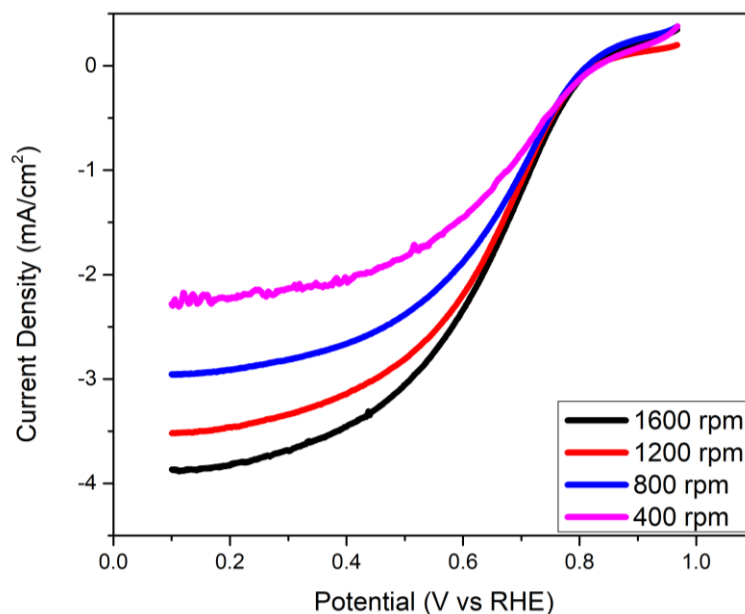


Figure 5- 7 LSV measurements of CuPt/NC at different rpms

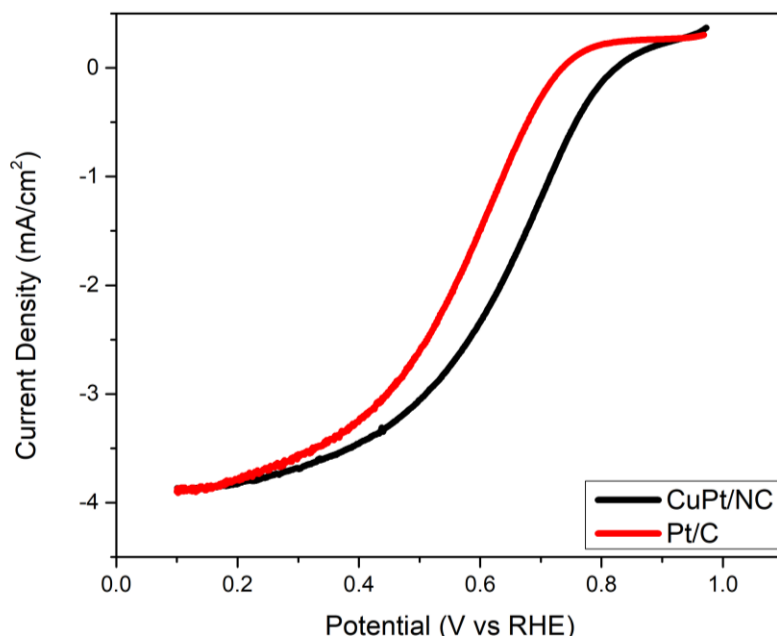


Figure 5- 8 LSV plots of CuPt/NC and commercial Pt/C at 1600 rpm with O₂ saturation

Commercial Pt/C and CuPt/NC was compared by LSV measurements (in HClO₄ with O₂ sat. at 1600rpm).CuPt/NC showed better ORR performance in terms of onset potential as shown in Figure 5-8. The Pt loading into the electrocatalyst clearly improved the ORR activity as the onset potential for CuPt/NC and Cu/NC is 0.9V (vs. RHE) and 0.2V (vs. RHE) (K-L plots and electron transfer number).

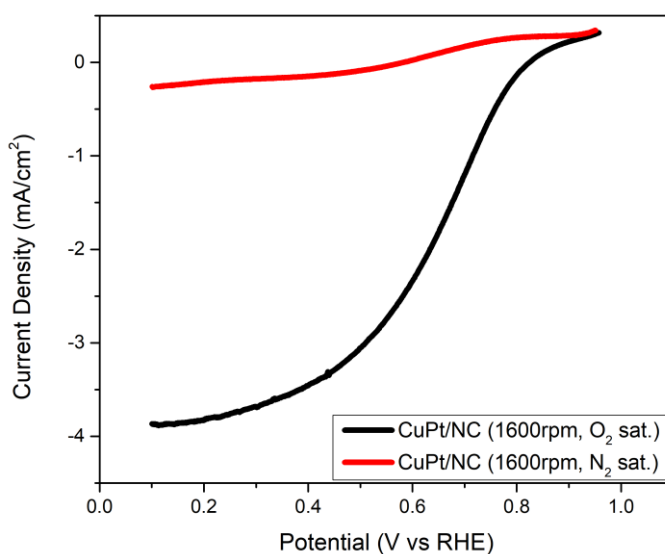


Figure 5- 9 LSV measurements of CuPt/NC with O₂ and N₂ 1600rp

In Figure 5-10 the comparison of Cu/NC and CuPt/NC is done by LSV, LSV was done in 0.1M HClO₄ with oxygen saturation at 1600rpm. Without the Pt loading the Cu/NC shows very poor performance for ORR but with Pt loading CuPt/NC showed excellent ORR performance. Pt and Cu combined give synergistic effect which improve the ORR performance.

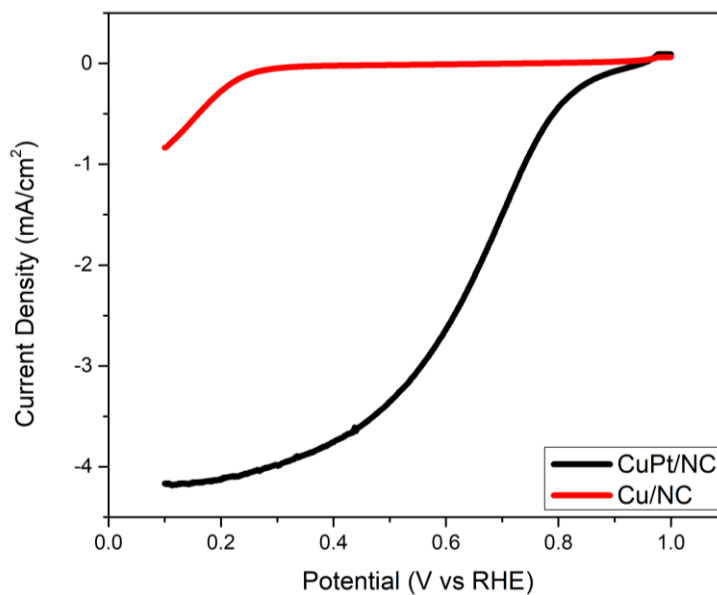


Figure 5- 10 LSV plots of Cu/NC and CuPt/NC

Electrochemical impedance spectroscopy (EIS) is another technique to determine the electrochemical activity of modified electrode. The nyquist plots in the Figure 5-11 shows that the charge transfer resistance for CuPt/NC is less than that of commercial Pt/C [6].

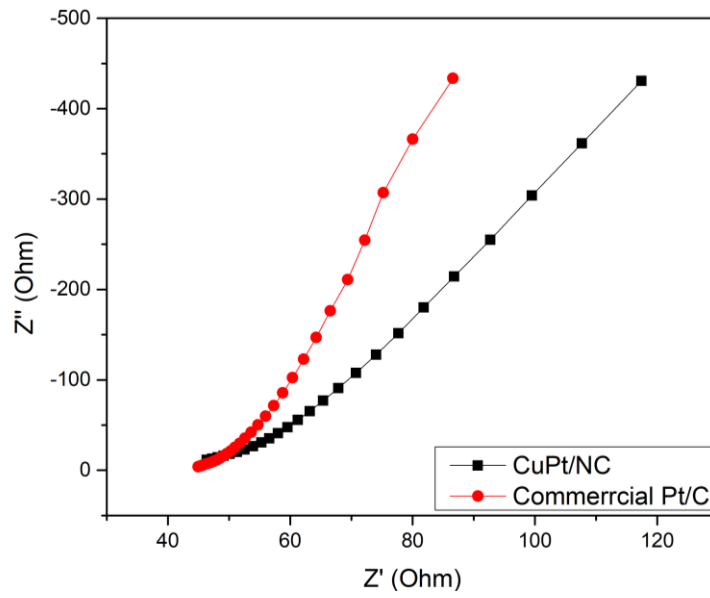


Figure 5- 11 The nyquist plots of CuPt/NC and commercial Pt/C

Summary

This chapter covers the overall characterization and electrochemical testing of the prepared electrocatalyst (CuPt/NC). SEM images reveals the formation of nanoporous carbon, while TEM shows the uniform distribution of CuPt nano particles. XRD and XPS graphs confirms the presence of Pt and alloy formation of CuPt because of shift in electronic states. CV and LSV measurements of CuPt/NC is compared with commercial Pt/C, and it is concluded that CuPt/NC has comparable performance for ORR that that of commercial Pt/C. CuPt/NC shows onset potential of 0.9V (vs. RHE) and halfwave potential of 0.79V (vs. RHE).

References

- [1] B. Y. Xia, Y. Yan, N. Li, H. Bin Wu, X. W. D. Lou, and X. Wang, "A metal-organic framework-derived bifunctional oxygen electrocatalyst," *Nat. Energy*, vol. 1, no. 1, pp. 1–8, 2016.
- [2] X. Shi, N. Iqbal, S. S. Kunwar, G. Wahab, H. A. Kasat, and A. M. Kannan, "Pt Co @ NCNTs cathode catalyst using ZIF-67 for proton exchange membrane fuel cell ScienceDirect Pt e Co @ NCNTs cathode catalyst using ZIF-67 for proton exchange membrane fuel cell," *Int. J. Hydrogen Energy*, no. October, 2017.
- [3] D. Wang *et al.*, "Electronic behaviour of Au-Pt alloys and the 4f binding energy shift anomaly in Au bimetallics-X-ray spectroscopy studies," *AIP Adv.*, vol. 8, p. 65210, 2018.
- [4] E. J. Coleman, M. H. Chowdhury, and A. C. Co, "Insights into the oxygen reduction reaction activity of Pt/C and PtCu/C catalysts," *ACS Catal.*, vol. 5, no. 2, pp. 1245–1253, 2015.
- [5] V. Vij, J. N. Tiwari, W. G. Lee, T. Yoon, and K. S. Kim, "Hemoglobin-carbon nanotube derived noble-metal-free Fe 5 C 2-based catalyst for highly efficient oxygen reduction reaction," *Sci. Rep.*, vol. 6, no. February, pp. 2–10, 2016.
- [6] R. Mehek, N. Iqbal, T. Noor, H. Nasir, Y. Mehmood, and S. Ahmed, "Novel Co-MOF/Graphene Oxide Electrocatalyst for Methanol Oxidation," *Electrochim. Acta*, vol. 255, no. January, pp. 195–204, 2017.

Chapter 6 Conclusion and Recommendations

6.1 Conclusion

The objective of the study was to develop a low Pt loaded electrocatalyst for ORR by using non-noble metals (Cu) in the form of their metal organic frameworks.

- Cu-MOF derived CuPt/NC (10%Pt loading) electrocatalyst for ORR was synthesized successfully.
- The pyrolysis of simple Cu-tpa MOF yields Cu/NC which has very low ORR activity while the pyrolysis of Cu-tpa MOF after Pt loading yields CuPt/NC which has very high ORR activity.
- The SEM and TEM of CuPt/NC reveal the formation of nano-porous carbon onto the surface of Cu-tpa MOF after pyrolysis. This nano-porous carbon plays an important role in electrochemical applications.
- XPS and XRD confirm the presence of Pt in CuPt/NC.
- Cyclic voltammetry of CuPt/NC shows that this novel catalyst has better ORR performance than that of commercial Pt/C.
- LSV indicates that CuPt/NC has onset potential of 0.9 V (vs. RHE) and half wave potential of 0.79 V (vs. RHE). Furthermore the limiting current of CuPt/NC is $4\text{mA}/\text{cm}^2$.

6.2 Recommendations

- Other non-noble metals can be used as an efficient ORR catalyst when combined with Pt.
- Metal organic frameworks are potential precursors for electrocatalysts.
- Bi-metallic MOFs can also be used to enhance ORR electrocatalyst.

Acknowledgments

All praise to the great Allah Almighty who made me the much capable that I could carry out this study and who enabled me to fulfill the obligation to explore the world of science up to my maximum limits.

I would like to express my sincere gratitude to my research supervisor Dr. Naseem Iqbal for his motivation, continuous support, patience and immense knowledge. He has guided me completely through-out my research work. I am also really thankful to my GEC members, Dr. M. Zubair, Dr. Nadia Shahzad, and Dr. Majid Ali for sparing precious time from their busy schedules, for suggestions as well as moral support. It an honor to be an exchange beneficiary and ambassador of Pakistan in Arizona State University, USA, so, I must be very thankful to USAID for giving me the opportunity to explore the American culture and academic system.

. A special thanks to lab engineers at Synthesis lab, AEMS lab and Combined lab Muhammad Naveed Ahmad, Asgar Ali, Aamir Satti, Haider Ijaz and Qamar-ud-Din who helped me a lot in the experimental work and testing.

Last but not the least, I would pay my regards to my family for their support and encouragement throughout my research work and my friends Unza Jamil, M. Ali, Syed Aun Rizvi, Asaad Iftekhar, Maria kanwal, Rida Mansoor, Daarain Haider, Wajeha Tauqir, Wajiha Ateeq, Leena Aftab and Saadia Hanif to accompany me in this journey.

Low Platinum loaded Cu-MOF derived electrocatalyst for oxygen reduction reaction in PEM fuel cell

Rehan Anwar^{1,2}, Saadia Hanif^{1,2}, Naseem Iqbal^{1*}, Xuan Shi², Daarain Haider¹, Syed Aun M.¹Tayyaba Noor³, A. M. Kannan²

¹USPCAS-E, National University of Sciences and Technology, Islamabad 44000, Pakistan

²Fuel Cell Laboratory, The Polytechnic School, Ira A. Fulton Schools of Engineering, Arizona State University, Mesa, AZ 85212, USA

³SCME, National University of Sciences and Technology, Islamabad 44000, Pakistan

Abstract

Metal-organic frameworks (MOFs) have received special attention in the recent past because of their structural properties and wide applications in catalysis. MOFs are also used as hard templates for the preparation of catalysts. In this study, highly active CuPt/NC electrocatalyst was synthesized by pyrolyzing Cu-tpa MOF along with Pt precursor under flowing Ar-H₂ atmosphere. The catalyst was characterized by scanning electron microscopy (SEM), transmission electron microscopy (TEM), X-ray photoelectron spectroscopy (XPS) and X-ray Powder Diffraction (XRD). Rotating disk electrode study was performed to determine the oxygen reduction reaction (ORR) activity for CuPt/NC in 0.1 M HClO₄ at different rotation per minute (400, 800, 1200 and 1600) and also compared with commercial Pt/C catalyst. Further the ORR performance was evaluated by K-L plots and tafel slope. CuPt/NC shows excellent ORR performance with onset potential of 0.9V (Vs. RHE), which is comparable with commercial Pt/C. The ORR activity of CuPt/NC exhibited it as an efficient electrocatalyst for fuel cell technology.

Keywords: Cu-tpa MOF; PEMFC ORR electrocatalyst; CuPt/NC; Platinum
* Corresponding Authors: Naseem Iqbal naseem@uspcase.nust.edu.pk

Introduction

Fossil fuels are not clean form of energy, they cause serious environmental damage. Secondly these fossil fuels are depleting day by day. So the world's energy generation is going through a transition from fossil fuels to clean and renewable energy resources [1]. Fuel cell converts chemical energy of fuel (H₂, Methanol, etc.) directly into electrical energy. Proton exchange membrane fuel cell (PEMFC) is an efficient and clean energy conversion device as it uses hydrogen as fuel. PEMFC can be used in both stationary as well as portable applications because of their high power density, low temperature operation as compared to other fuel cells [2][3][4]. Pt based electrocatalyst are used for oxygen reduction reaction (ORR) due to their high activity. So far the limited commercialization of PEMFC is associated with the high cost and durability of Pt catalyst [5]. Currently there are a lot of efforts are being made to minimize the use of Pt catalyst in PEMFC. Oxygen reduction reaction (ORR) is very crucial in PEMFC as it limits the current density which as a results affects the overall fuel cell performance. So, ORR has to be faster and efficient. The ORR kinetics can be improved by alloying noble metals (Pt, Pd) with Cu, Ni, Co and Fe [6] [7] [8].

Metal-organic frameworks (MOFs) have been proved as emerging and advanced materials for multiple applications especially in catalysis because of their highly porous structures[9][10] [10]. MOFs have also been used as precursors for synthesis of nanocomposites. They have micro-pores and low graphitic degree which is not desirable for electrochemical activity. The pyrolysis of MOFs can be used to create highly porous

structures which are stable at higher temperature and have much higher electrochemical activity [11][12][13]. Rui Wang and co-workers designed a porous carbon matrix with phosphorous and nitrogen doping using Cu-MOF, this catalyst exhibited a remarkable performance as a bi-functional electrocatalyst for ORR and HER [14].

In the present study, a novel electrocatalyst for ORR was successfully synthesized by pyrolysis of Cu-MOF with very low Pt loading. This Cu-MOF derived electrocatalyst has nano-porous carbon (NC) formed in it. The ORR performance of the CuPt/NC is compared with commercial Pt/C.

2. Experimental

2.1 Synthesis of Cu-tpa MOF.

Cu-tpa MOF was synthesized by method described in the literature [15]. In a typical synthesis 5mg of $\text{CuNO}_3 \cdot 3\text{H}_2\text{O}$ was dissolved in deionized (DI) water, 2mg of terephthalic acid was dissolved in mixed solution of 40ml N,N-dimethyl formaldehyde (DMF) and 40ml of ethanol. Both the above mentioned solutions (containing $\text{CuNO}_3 \cdot 3\text{H}_2\text{O}$ and terephthalic acid) were mixed together and placed on hot plate at 80°C for 24h. The blue powder was centrifuged and washed with DMF and DI water. The collected powder was dried at 80°C in a vacuum oven.

2.2 Synthesis of CuPt/NC.

100mg of Cu-tpa MOF was mixed with 0.1ml of 96.5mM H_2PtCl_6 and the mixture was dried at 80°C for 2 h. The dried powder was heated to 350°C for 1.5 h then heated to 700°C at the ramp rate of $2^\circ\text{C}/\text{min}$ and kept it at 700°C for 3.5 h under the constant flow of Ar- H_2 (90% Ar) in the tube furnace. After cooling down the furnace temperature naturally the black pyrolyzed powder was collected. After the acid wash the resultant catalyst with

<10%Pt loading was recovered after centrifugation, multiple washings with DI water and drying at 80°C in vacuum oven. Cu/NC was synthesized by the same method without Pt loading.

2.3 Catalyst Characterization

SEM images were taken on VEGA3 TESCON at 20KV, at different magnifications. EDS was also performed along with SEM on the same machine. Siemens D5000 Powder X-ray Diffractometer was used to identify the crystal structure. XRD data is collected between the 2θ values of 10°-90° for CuPt/NC and Cu $K\alpha$ was used as an X-ray source. Transmission electron microscopy (TEM) was done on CM200-FEG (Philips) at 200 keV. The XPS was performed on VG 220i-XL.

2.4 Catalyst ink and electrode preparation

Catalyst ink was prepared by dissolving 2 mg of catalyst (Cu/NC, CuPt/NC and Pt/C) in 1 ml of stock solution and sonicated the suspension in ultrasonic bath for 30 min (commercial Pt/C catalyst used was 46.1 wt% from Tanaka Kikinzoku Kogyo, TEC10E50E). Stock solution was prepared by mixing together 7.6 ml of DI water, 2.4 ml of iso-propyl alcohol and 0.1 ml of 5 wt % nafion dispersion (Ion power LQ-1105 - 1100 EW) [16]. The catalyst electrode film was prepared on glassy carbon (with diameter of 5mm from Pine Research AFE5T050GC) by dropping 10 μ m of ink on it and dried it for 20 min at 700 rpm. The thin films of Commercial Pt/C and Cu/NC were also deposited for comparison purpose.

2.6 Electrochemical Evaluation

CV and LSV measurements were taken on three electrode system in 0.1 M HClO₄ with N₂ and O₂ purging (for 20-30 min) [17]. Voltage window for LSV experiments were from 0.7 to 0.3 V against SCE (that is 1 to 0 V against RHE). Pt coil was used as counter electrode and Ag/AgCl electrode (in 3M KCl) was used as reference electrode. All the electrochemical were conducted at voltage scan rate of 30 mVs⁻¹.

3. Results and Discussion

Fig.1 shows SEM images with identical magnification for Cu-tpa MOF before and after pyrolysis. The Cu-tpa MOF particle size is around 400nm, these particles do not possess specific regular shape but shows a good crystallinity [15]. After the pyrolysis the sample was changed into a black powder because of the carbonization of organic linker. During the process of pyrolysis the Cu-tpa MOF decomposes partially as the unstable organic groups evaporate and leaving only the carbon behind. It is observed from Fig.1 b,c the formation of nano-porous carbon onto the surface Cu-tpa particles and with Pt loading surface became rougher and porous.

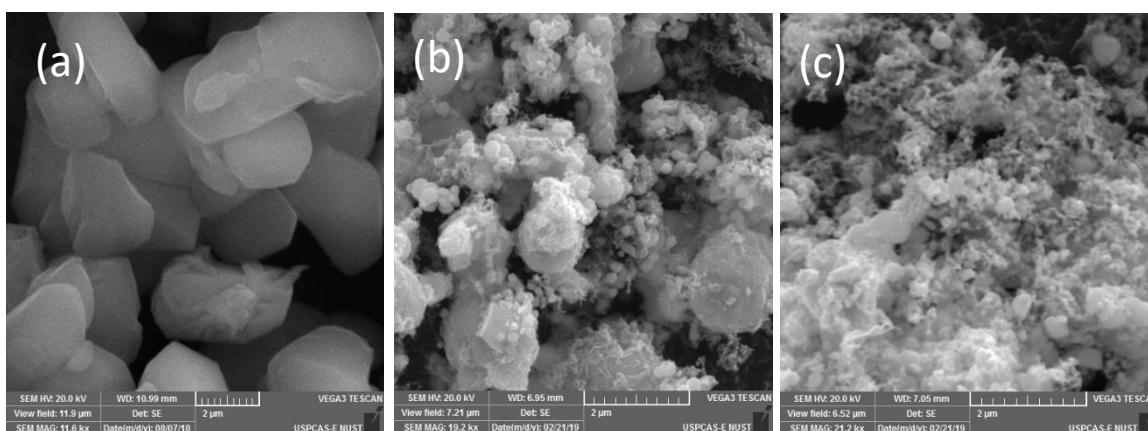


Figure 1 Scanning electron microscopy images of (a) Cu-tpa MOF (b) Cu/NC (c) CuPt/NC

Fig 2. Shows the EDS data peaks of all three samples including Cu-tpa MOF, Cu/NC and CuPt/NC. Carbon, oxygen and copper peaks are seen in all three samples EDS results while the Pt peak is observed only in CuPt/NC. Moreover the elemental percentages from EDS are shown in the Table 1. Cu-MOF has highest percentage of carbon while the other two pyrolyzed samples have relatively lower percentage of carbon as the unstable organic groups have evaporated after pyrolysis which also decreases the carbon percentage. The

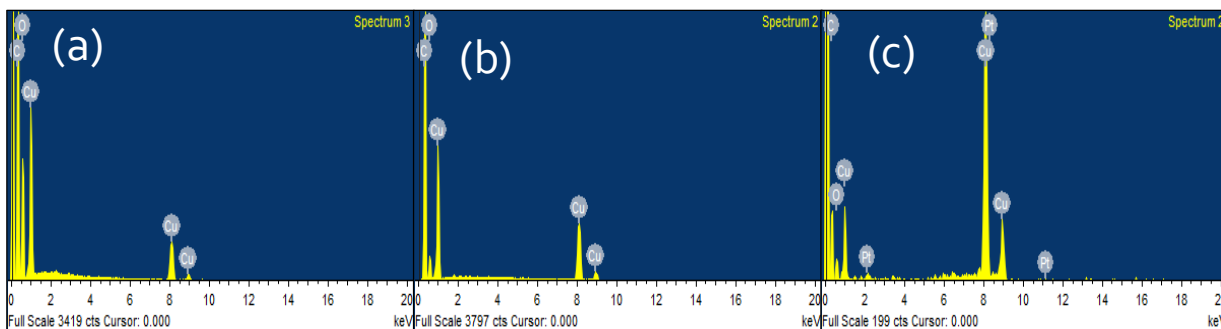


Figure 2 Energy dispersive X-ray spectroscopy (a) Cu-tpa MOF (b) Cu/NC (c) CuPt/NC

	Cu-tpa MOF		Cu/NC		CuPt/NC	
Element	Weight%	Atomic%	Weight%	Atomic%	Weight%	Atomic%
C	57.05	67.34	66.88	85.16	51.01	79.14
O	34.80	30.84	9.60	9.18	8.01	9.20
Cu	8.15	1.82	23.51	5.66	39.95	11.65
Pt	-	-	-	-	1.03	-
Totals	100.00		100.00		100.00	

Table 3 Atomic and weight percentage in EDS analysis

In Fig 3. TEM images of CuPt/NC have shown at two different magnifications of 20nm and 10nm, from the TEM images it is observed that the pyrolyzed sample contains numerous small CuPt NP distributed uniformly on carbon matrix. The size of CuPt/NC is around 4-5nm.

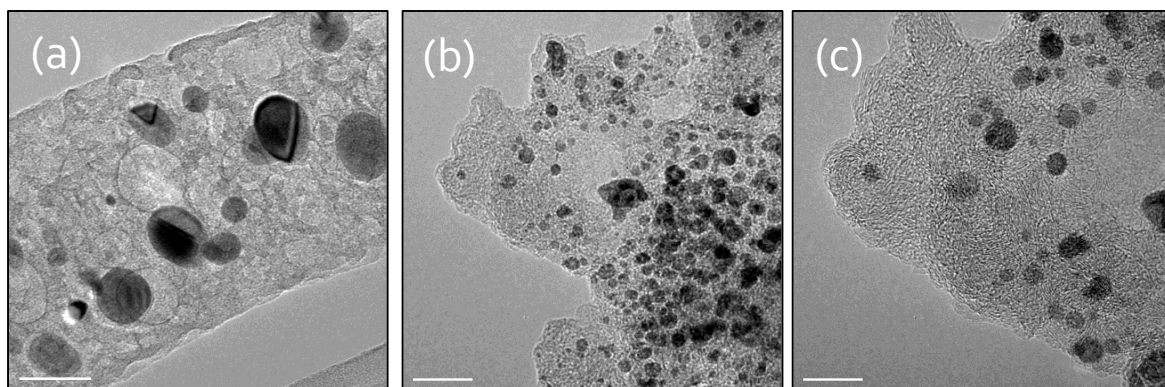


Figure 3 Transmission electron micrographs for CuPt/NC (a) 50nm (b) 20nm (c) 10nm

The XRD graph of CuPt/NC shows sharp peak of Cu (111) at 50.7° and Cu (200) at 59.2° . A little hump between $25-30^\circ$ indicates nano-porous carbon. XRD peak of Pt (111) was observed at 2-theta of 45.2° along with little diffraction of Pt (220) at 80.39° (Fig. 4).

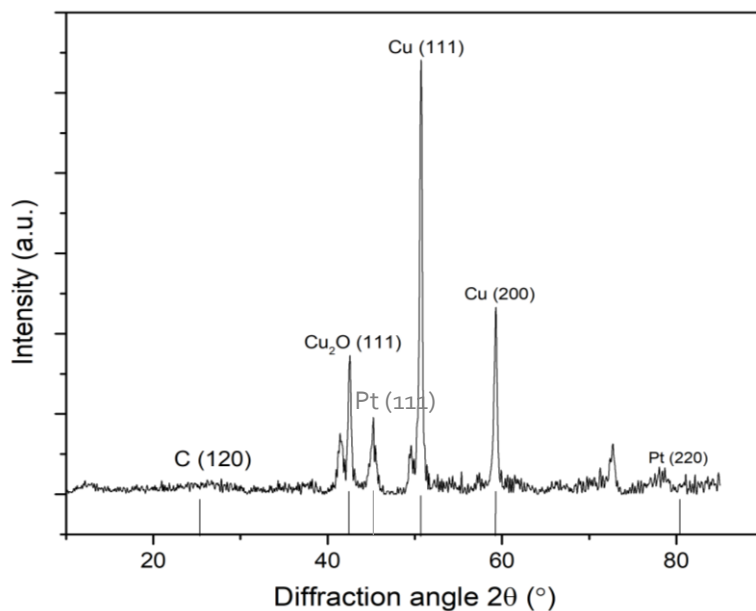


Figure 4 XRD pattern of CuPt/NC with (hkl) values

Fig. 5 displays the XPS spectra of CuPt/N which confirms the same surface composition as that of bulk. XPS further confirms the presence of Pt. A positive electronic shift of 1.45eV (72.45-71eV) and 0.46eV (933-933.46eV) in Pt (4f) and Cu (2p) respectively is considered because of Cu-Pt metal interaction and the formation of CuPt nanoparticles [18] [19]. C (1s) peak at ~286eV and O (1s) peak at 530.8eV attribute to C-O-C and C-O components respectively [20].

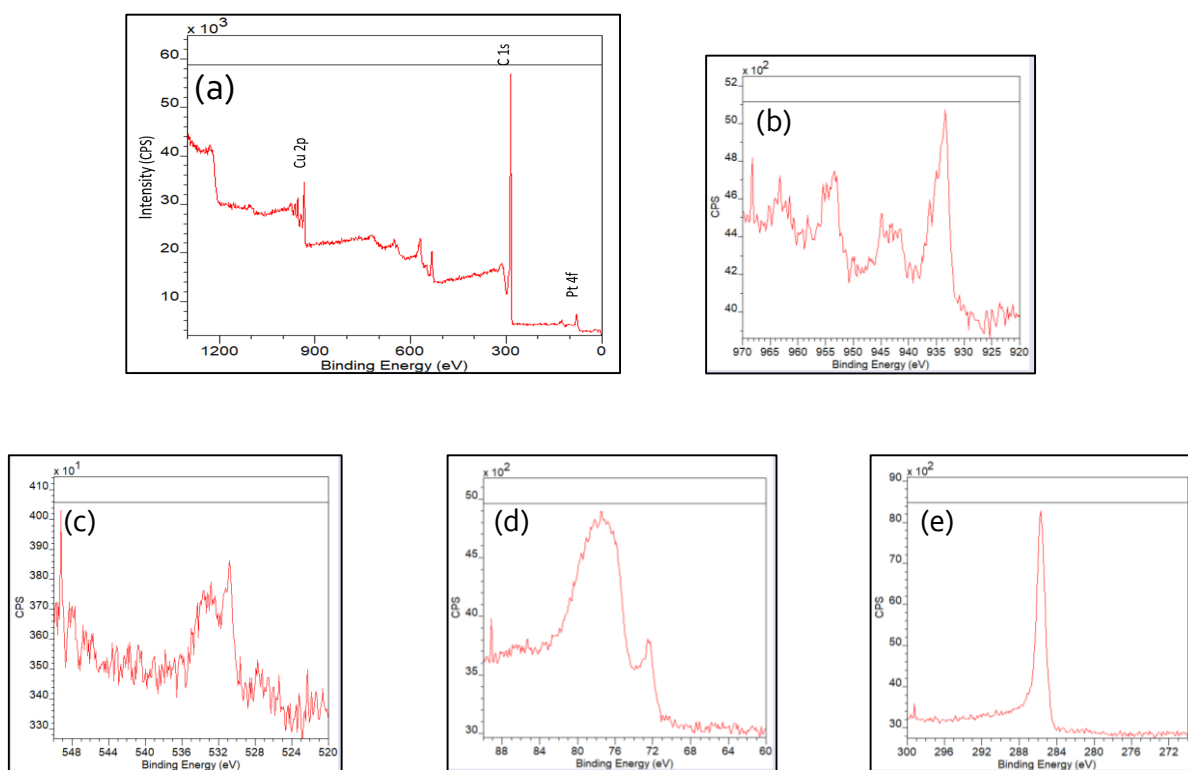


Figure 5 (a) XPS wide spectrum of CuPt/NC and individual XPS scans of (b) Cu2p (c) O1s (d) Pt4f (e) C1s

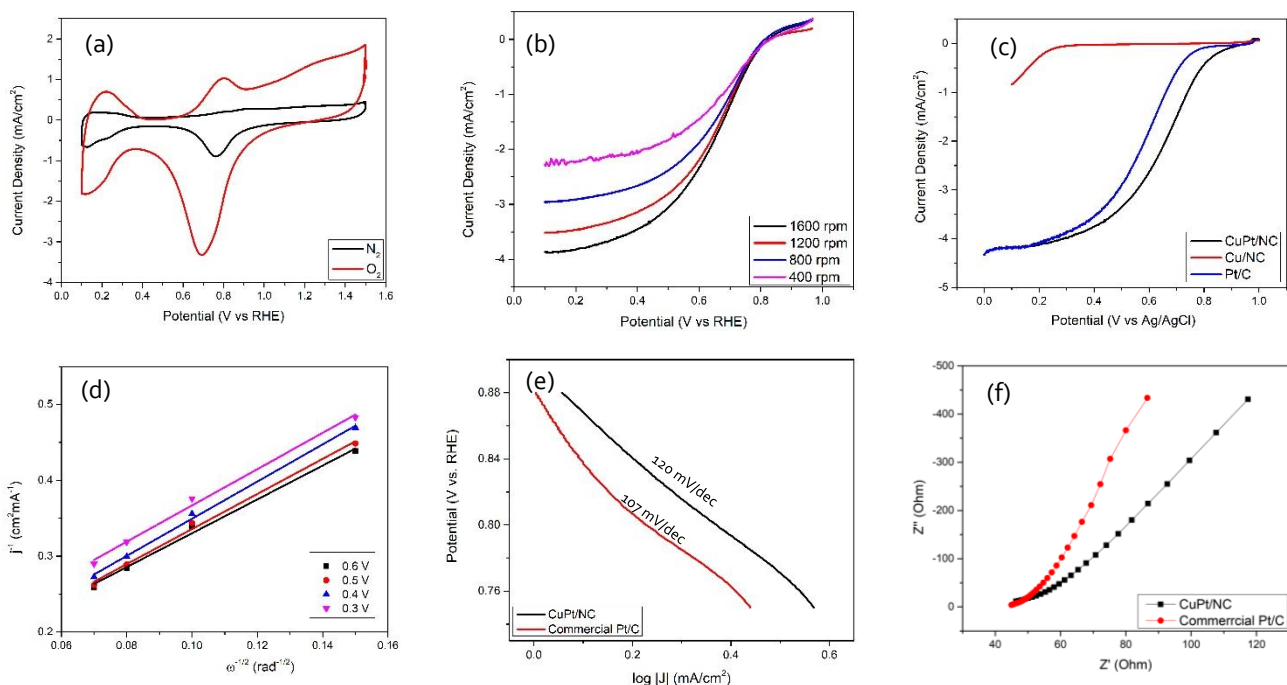


Figure 6 Evaluation of ORR activity for CuPt/NC **a**) CV plots (with nitrogen and oxygen saturation 0.1M HClO₄ solution). **b**) LSV plots at different rotation rates (rpm) for CuPt/NC **c**) Comparison of LSV curves of Cu/NC, CuPt/NC and Pt/C with O₂ saturation in 0.1M HClO₄ solution at 1600 rpm. **d**) K–L plots from 0.6V to 0.3V, ω is the angular rotation speed. **e**) Tafel slope comparison of CuPt/NC and Pt/C **f**) Nyquist plots for CuPt/NC and Pt/C

For the electrochemical testing of CuPt/NC, First the cyclic voltammetry (CV) was performed in 0.1M HClO₄ with nitrogen saturation no significant oxygen reduction peak was observed, with oxygen saturation a distinct peak at a potential of 0.7V is observed which is oxygen reduction reaction peak (Fig. 6.a). Further ORR activity of CuPt/NC is evaluated by linear sweep voltammetry (LSV) measurements taken at different rotations using rotating disk electrode system (RDE), which displays that CuPt/NC has limiting current of 4 mA/cm² at 1600rpm (Fig. 6.b). ORR activity of CuPt/NC is compared with commercial Pt/C and CuP/NC. CuPt/NC has the highest onset potential of 0.9V while it is 0.85V the commercial Pt/C and the Cu/NC has very low onset potential of 0.26V. So CuPt/NC has 50mV more positive onset potential than that of commercial Pt/C (Fig. 6.c).

ORR kinetics is analyzed by Koutecky-Levich (K-L) equation, linear K-L plots in Fig. 6.d represents the first order reaction kinetics for ORR. The electron transfer number (n) is calculated using K-L plots and it lies in between 3.93-3.97 for the voltage range of 0.3-0.6 V [21], charge transfer number for commercial Pt/C is 4.00, as it follows 4e pathway for ORR, so the n calculated for CuPt/NC is close to 4.00 so it also follows 4e pathway [22]. Furthermore the closer values of Tafel slopes for CuPt/NC and Pt/C confirms the same reaction mechanisms as Tafel slope for CuPt/NC is 107 mV/dec on the other hand for Pt/C it is 120 mV/dec (Fig. 6.e) The lower Tafel slope of CuPt/NC shows that it has higher ORR activity than Pt/C [23] [24]. Electrochemical impedance spectroscopy (EIS) is also used to determine the electrochemical activity of modified electrode. Charge transfer resistance is measured from nyquist plots, the lower slope of the plot represents the lower charge transfer resistance. Fig. 7.f shows the nyquist plots of CuPt/NC exhibits lower slope than Pt/C which translated as the charge transfer resistance for CuPt/NC is less than that of commercial Pt/C [25]. The overall ORR performance comparison of CuPt/NC and Pt/C along with kinetics parameters has shown in Table 3.

Table 4 Over all ORR performance comparison of CuPt/NC and Pt/C

Electrochemical properties	CuPt/NC	Pt/C
Onset potential	0.9V (vs. RHE)	0.8V (vs. RHE)
Peak current density	4.5 mA/cm ²	3.32 mA/cm ²
Tafel slope	107 mV/dec	120 mV/dec
Electron transfer number	~4	4
Diffusion co-efficient	8.51 *10 ⁻³	6.28*10 ⁻³
Charge transfer co-efficient	0.027 cm ² sec ⁻¹	0.3 cm ² sec ⁻¹

4. Conclusions

In this work, we synthesized a highly active and efficient CuPt/NC an ORR catalyst, derived from Cu-MOF. SEM showed that Pt loading results in the increased formation of nanoporous carbon. TEM images display uniform of CuPt nanoparticles. Shift in binding energy of Cu2p and Pt4f in XPS is interpreted as Cu-Pt interaction. The onset potential of CuPt/NC is 0.9V (vs. RHE) and the value of limiting current density is 4mA/cm², furthermore linearity of K-L plots and the charge transfer number value of 3.93-3.97 indicated single step kinetics. Tafel slope also shows that CuPt/NC and commercial Pt/C follows the same reaction kinetics. From EIS studies It was concluded that CuPt/NC has lower charge transfer resistance than Pt/C. Hence the results prove CuPt/NC as a potential ORR catalyst.

References

- [1] Y. Wang, K. S. Chen, J. Mishler, S. C. Cho, and X. C. Adroher, "A review of polymer electrolyte membrane fuel cells: Technology, applications, and needs on fundamental research," *Appl. Energy*, vol. 88, no. 4, pp. 981–1007, 2011.
- [2] B. Y. Xia *et al.*, "oxygen electrocatalyst," vol. 1, no. January, pp. 1–8, 2016.
- [3] J. Suntivich, H. A. Gasteiger, N. Yabuuchi, H. Nakanishi, J. B. Goodenough, and Y. Shao-horn, "Design principles for oxygen-reduction activity on perovskite oxide catalysts for fuel cells and metal–air batteries," *Nat. Publ. Gr.*, vol. 3, no. 8, p. 647, 2011.
- [4] W. R. W. Daud, R. E. Rosli, E. H. Majlan, S. A. A. Hamid, R. Mohamed, and T. Husaini, "PEM fuel cell system control: A review," *Renew. Energy*, vol. 113, pp. 620–638, 2017.
- [5] M. Kiani *et al.*, "Recent developments in electrocatalysts and future prospects for oxygen reduction reaction in polymer electrolyte membrane fuel cells," *J. Energy Chem.*, vol. 27, no. 4, pp. 1124–1139, 2018.
- [6] T. Jensen and K. Schmainda, "Standardization of rCBV values improves tumor contrast," *Proc. 14th Sci. Meet. Int. Soc. Magn. Reson. Med.*, p. 3493, 2006.
- [7] "Li – O₂ and Li – S batteries with high energy storage," vol. 11, no. FEBRUARY, p. 3237, 2012.
- [8] M. Wang, "Novel nanostructured electrocatalysts for fuel cells," 2015.
- [9] H. Wang, Q. Zhu, R. Zou, and Q. Xu, "Metal-Organic Frameworks for Energy

- Applications,” *CHEMPR*, vol. 2, no. 1, pp. 52–80, 2017.
- [10] J. Lee, O. K. Farha, J. Roberts, K. A. Scheidt, S. T. Nguyen, and J. T. Hupp, “2009 Metal – organic frameworks issue Metal – organic framework materials as catalysts w,” no. 5, 2009.
- [11] X. Shi, N. Iqbal, S. S. Kunwar, G. Wahab, H. A. Kasat, and A. M. Kannan, “Pt Co @ NCNTs cathode catalyst using ZIF-67 for proton exchange membrane fuel cell ScienceDirect Pt e Co @ NCNTs cathode catalyst using ZIF-67 for proton exchange membrane fuel cell,” *Int. J. Hydrogen Energy*, no. October, 2017.
- [12] E. Antolini, “Nitrogen-doped carbons by sustainable N- and C-containing natural resources as nonprecious catalysts and catalyst supports for low temperature fuel cells,” *Renew. Sustain. Energy Rev.*, vol. 58, pp. 34–51, 2016.
- [13] K. Sumida *et al.*, “Carbon Dioxide Capture in Metal À Organic Frameworks,” pp. 724–781, 2012.
- [14] R. Wang, X. Dong, J. Du, J. Zhao, and S. Zang, “MOF-Derived Bifunctional Cu 3 P Nanoparticles Coated by a N , P-Codoped Carbon Shell for Hydrogen Evolution and Oxygen Reduction,” vol. 1703711, pp. 1–10, 2018.
- [15] X. Wang *et al.*, “Highly dispersible and stable copper terephthalate MOF-graphene oxide nanocomposite for electrochemical sensing application Highly dispersible and stable copper terephthalate MOF-graphene oxide nanocomposite for electrochemical sensing application,” 2014.
- [16] K. Shinozaki, J. W. Zack, R. M. Richards, B. S. Pivovar, and S. S. Kocha, “Oxygen

- Reduction Reaction Measurements on Platinum Electrocatalysts Utilizing Rotating Disk Electrode Technique I . Impact of Impurities , Measurement Protocols and Applied Corrections,” vol. 162, no. 10, pp. 1144–1158, 2015.
- [17] A. Schoonen and D. T. Rickard, “REMOVAL OF DISSOLVED OXYGEN FROM WATER : A COMPARISON OF FOUR COMMON TECHNIQUES,” vol. 41, no. 2, pp. 211–215, 1994.
- [18] H. Peng, W. Qi, H. Wu, J. He, Y. Li, and H. Xie, “RSC Advances One-pot synthesis of CuPt nanodendrites with,” *RSC Adv.*, vol. 8, pp. 9293–9298, 2018.
- [19] C. Poochai and N. Electronics, “CO,” no. December, 2016.
- [20] A. Ganguly, S. Sharma, P. Papakonstantinou, and J. Hamilton, “Probing the Thermal Deoxygenation of Graphene Oxide Using High-Resolution In Situ X-ray-Based Spectroscopies,” no. October, 2013.
- [21] R. Zhou, Y. Zheng, M. Jaroniec, and S. Qiao, “Determination of the Electron Transfer Number for the Oxygen Reduction Reaction: From Theory to Experiment,” vol. 4728, 2016.
- [22] Y. J. Sa, D. Seo, J. T. Lim, S. Korea, and D. Kang, “A General Approach to Preferential Formation of Active Fe-N_x Sites in Fe-N/C Electrocatalysts for Efficient Oxygen Reduction Reaction,” no. October, 2016.
- [23] M. Chiwata, K. Kakinuma, M. Wakisaka, and M. Uchida, “Oxygen Reduction Reaction Activity and Durability of Pt Catalysts Supported on Titanium Carbide,” no. June, 2015.

- [24] T. Shinagawa, A. T. Garcia-Esparza, and K. Takanahe, “Insight on Tafel slopes from a microkinetic analysis of aqueous electrocatalysis for energy conversion,” *Sci. Rep.*, vol. 5, no. August, pp. 1–21, 2015.
- [25] R. Mehek, N. Iqbal, T. Noor, H. Nasir, Y. Mehmood, and S. Ahmed, “Novel Co-MOF/Graphene Oxide Electrocatalyst for Methanol Oxidation,” *Electrochim. Acta*, vol. 255, no. January, pp. 195–204, 2017.